Epigenetic displacement of HP1 from heterochromatin by HIV-1 Vpr causes premature sister chromatid separation

Mari Shimura,[1] Yusuke Toyoda,[2] Kenta Iijima,[1] Masanobu Kinomoto,[3] Kenzo Tokunaga,[3] Kinya Yoda,[4] Mitsuhiro Yanagida,[2] Tetsutaro Sata,[3] and Yukihito Ishizaka[1]

[1]Department of Intractable Diseases, Research Institute, National Center for Global Health and Medicine, Shinjuku, Tokyo 162-8655, Japan
[2]Department of Gene Mechanisms, Graduate School of Biostudies, Kyoto University, Sakyou-ku, Kyoto 606-8501, Japan
[3]Department of Pathology, National Institute of Infectious Diseases, Shinjuku, Tokyo 162-8640, Japan
[4]Bioscience Biotechnology Center, Nagoya University, Nagoya 464-8601, Japan

Although pericentromeric heterochromatin is essential for chromosome segregation, its role in humans remains controversial. Dissecting the function of HIV-1–encoded Vpr, we unraveled important properties of heterochromatin during chromosome segregation. In Vpr-expressing cells, hRad21, hSgo1, and hMis12, which are crucial for proper chromosome segregation, were displaced from the centromeres of mitotic chromosomes, resulting in premature chromatid separation (PCS). Interestingly, Vpr displaced heterochromatin protein 1-α (HP1-α) and HP1-γ from chromatin. RNA interference (RNAi) experiments revealed that down-regulation of HP1-α and/or HP1-γ induced PCS, concomitant with the displacement of hRad21. Notably, Vpr stimulated the acetylation of histone H3, whereas p300 RNAi attenuated the Vpr-induced displacement of HP1-α and PCS. Furthermore, Vpr bound to p300 that was present in insoluble regions of the nucleus, suggesting that Vpr aberrantly recruits the histone acetyltransferase activity of p300 to chromatin, displaces HP1-α, and causes chromatid cohesion defects. Our study reveals for the first time centromere cohesion impairment resulting from epigenetic disruption of higher-order structures of heterochromatin by a viral pathogen.

Introduction

The scheduled separation of chromosomes is crucial for balanced chromosome segregation. A cohesin complex keeps sister chromatids held together until the onset of anaphase (Nasmyth, 2002; Yanagida, 2005). If centromeric cohesion is impaired, sister chromatids separate before anaphase, resulting in premature chromatid separation (PCS; Kitajima et al., 2006; Toyoda and Yanagida, 2006). We previously reported that PCS occurs in the peripheral blood lymphocytes (PBLs) of HIV-1–infected individuals (Shimura et al., 2005). Strikingly, in vitro HIV-1 infection induced PCS in PBLs isolated from healthy humans, strongly suggesting that a viral factor was responsible for PCS. As PCS has been associated with aneuploidy, it is important to identify the mechanisms involved (Thompson et al., 1993; Zhu et al., 1995; Kajii et al., 2001).

Centromere cohesion is regulated by a cohesin complex, which consists of four evolutionarily conserved subunits: the structural maintenance of chromosome (SMC) proteins Smc1 and Smc3 and the non-SMC proteins Scc3/SA and Scc1/Rad21/kleisin (Hirano, 2005). During mitosis, cohesin complexes at the chromosome arm are released non-proteolytically in a process mediated by Aurora B (AurB) and Pololike kinase 1 (Losada et al., 2002; Sumara et al., 2002; Giménez-Abián et al., 2004). In contrast, centromeric

M. Shimura and Y. Toyoda contributed equally to this paper.

Correspondence to Mari Shimura: mshimura@ri.ncgm.go.jp

Y. Toyoda's present address is Max Planck Institute of Molecular Cell Biology and Genetics, 01307 Dresden, Germany.

Abbreviations used in this paper: AA, anacardic acid; ACA, anticentromere antibody; AurB, Aurora B; CPC, chromosomal passenger complex; CSK, cytoskeleton; DOX, doxycycline; HAT, histone acetyltransferase; HDAC, histone deacetylase; INCENP, inner centromere protein; LR, leucine/arginine rich; LTR, long terminal repeat; PBL, peripheral blood lymphocyte; PCS, premature chromatid separation; SMC, structural maintenance of chromosome; VSV-G, vesicular stomatitis virus glycoprotein; wt, wild type.

The Rockefeller University Press $30.00
J. Cell Biol. Vol. 194 No. 5 721–735
www.jcb.org/cgi/doi/10.1083/jcb.201010118

cohesin is protected until the onset of anaphase by Shugosin (hSgo1; Kitajima et al., 2006). Importantly, previous observations suggested that cohesion is functionally linked to heterochromatin structure. For example, the degradation of *Drosophila melanogaster* heterochromatin protein 1 (HP1), which functions as a component of silent heterochromatin, causes unbalanced chromosome segregation (Kellum and Alberts, 1995). In fission yeast, Swi6, a homologue of HP1, is important for maintaining Scc1/Rad21 at the centromere until anaphase (Nonaka et al., 2002; Pidoux and Allshire, 2004). In humans, however, there is controversy regarding the regulation of centromeric cohesin complexes during mitosis by HP1, which exists as three subtypes: HP1-α, HP1-β, and HP1-γ. Inoue et al. (2008) reported that the dominant-negative form of HP1-β is involved in centromere cohesion. Previously, we showed that HP1-α RNAi induced hSgo1 mislocation, suggesting that HP1-α RNAi induced PCS (Yamagishi et al., 2008). In contrast, Mateos-Langerak et al. (2007) reported that no HP1 dominant-negative mutants showed detectable effects on the centromeric heterochromatin. Recently, Serrano et al. (2009) suggested that none of the three HP1 subtypes has a definite role in the loading of cohesion to chromatin.

Here, we found that *vpr*, an HIV-1 accessory gene, was responsible for HIV-1–associated PCS. The *vpr* gene encodes Vpr, a virion-associated nuclear protein (Cohen et al., 1990) that binds p300 and facilitates transcription from HIV-1 promoters (Felzien et al., 1998; Kino et al., 2002). Strikingly, we observed that Vpr reduced the levels of chromatin-associated HP1-α and HP1-γ and concomitantly triggered the displacement of hRad21, hSgo1, and an HP1-α/-γ–interacting protein, hMis12, all of which are critically involved in centromere cohesion and kinetochore functions (Goshima et al., 2003; Obuse et al., 2004). To investigate the molecular mechanisms underpinning Vpr-induced PCS, we examined the effects of HP1 RNAi and found that the down-regulation of HP1-α and/or HP1-γ induced PCS, coinciding with the displacement of hRad21 from centromeres. Additional experiments using p300/histone acetyltransferase (HAT) inhibitors and RNAi-based assays revealed that Vpr-induced PCS and the displacement of HP1-α from chromatin depended on the HAT activity of p300. Based on these data, we conclude that Vpr aberrantly modulates p300/HAT activity and induces PCS by causing defects in the higher-order structures of centromeric heterochromatin.

High rates of PCS have been reported in human diseases caused by mutations in genes essential for chromatid cohesion, including *ESCO2* and *NIPBL/Adherin*, which are responsible for Roberts syndrome and Cornelia de Lange syndrome, respectively (Kaur et al., 2005; Vega et al., 2005; Dorsett, 2007), and are involved in the spindle assembly checkpoint, including *Bub1* (Kajii et al., 2001). PCS is also observed in malignant cancers (Thompson et al., 1993; Zhu et al., 1995). Although the molecular mechanisms behind these pathological conditions remain unclear, our data indicate that centromere proteins are susceptible to disruption by the epigenetic modification of chromatin.

Results

Vpr is responsible for PCS caused by HIV-1

To identify the HIV-1 gene responsible for PCS, we infected human PBLs with wild-type (wt) or mutant viruses (*Δvpu*, *Δvpr*, and *Δvif*; Fig. 1 A, bottom). HIV-1 consists of nine ORFs containing three structural genes, *gag*, *pol*, and *env*, plus the regulatory genes *rev* and *tat*, together with four different accessory genes, *vif*, *vpr*, *vpu*, and *nef* (Fig. 1 A, top). In this study, we used vesicular stomatitis virus glycoprotein (VSV-G)–pseudotyped viruses lacking the *nef* gene to perform a single-round replication assay (Kinomoto et al., 2007) in which we introduced mutations only into accessory genes with no influence on the rate of infection (Malim and Emerman, 2008). As shown in Fig. 1 B, PCS was observed in cells infected with wt, *Δvpu*, and *Δvif* viruses but not by *Δvpr* virus (Fig. 1 C, left). We carefully examined >300 chromosome spreads in each experiment. A chromosome spread was considered PCS positive if more than three chromosomes lacked linkages between sister chromatids. We obtained similar results in two additional independent experiments (Fig. S1 A). Infection rates with a multiplicity of infection of 0.007 were comparable, as assessed by luciferase reporter activity (Fig. 1 C, right), suggesting that *vpr* is responsible for HIV-1–associated PCS. Next, we examined PCS in MIT-23 cells, which stably express Vpr under the control of a tetracycline-inducible promoter (Shimura et al., 1999). On day 2 after the addition of doxycycline (DOX), PCS was clearly detected in >40% of treated cells (Fig. 1 D, right) but not in control cells (Fig. 1 D, left). To characterize the dosage of Vpr in MIT-23 cells, its expression was compared with HIV-1–infected cells. The level of Vpr in DOX-treated MIT-23 cells was less than one seventh of that in virus-producing U1 cells, which are latently infected and carry two copies of provirus HIV-1 DNA (Fig. S1, B and C; Folks et al., 1987). Based on these data, we conclude that Vpr is responsible for the PCS induced by HIV-1 infection.

Consistent with studies linking PCS with aberrant segregation of sister chromatids (Babu et al., 2003; Sotillo et al., 2007; Zhang et al., 2008), numerous Vpr-expressing G_2/M phase cells displayed altered ploidy (Fig. 1 E). Time-lapse analysis revealed that mitosis was prolonged in Vpr-expressing cells (Fig. S1 D, right). Furthermore, >50% of the mitotic Vpr-expressing cells examined displayed abnormal mitosis (Fig. S1 D and Videos 1–3). Interestingly, Vpr-expressing cells suffered no apparent cellular crisis, as judged by FACS analysis of the sub-G1 population (Fig. 1 E) and increased aneuploidy (Fig. 1 E, arrow), which is consistent with our previous finding (Shimura et al., 1999).

Vpr causes cohesion defects primarily in mitosis

Because chromosome segregation is tightly controlled by centromeric cohesin (Nonaka et al., 2002; Pidoux and Allshire, 2004), we first investigated the expression of the cohesin subunits Smc1, Smc3, and Scc1/Rad21 in Vpr-expressing MIT-23 cells. 2 d after the induction of Vpr expression, the chromatin-enriched

insoluble fraction was isolated using a reported method (Todorov et al., 1995), and protein expression was assayed by immunoblotting. The amount of Smc1, Smc3, and Scc1/hRad21 proteins in the isolated chromatin decreased by 79, 58, and 53%, respectively (Fig. 2 A, top). In striking contrast, the levels of these proteins in whole-cell extracts remained stable (Fig. 2 A, bottom), suggesting that Vpr altered their subcellular localization. To focus on cohesin localizing to condensed chromosomes, we prepared chromosome spreads from Vpr-expressing cells and stained them with an antibody against hRad21 (Hoque and Ishikawa, 2002). As shown in Fig. 2 B, only small amounts of hRad21 were observed in the spreads, in which sister chromatids were aligned loosely as a result of PCS (Fig. 2 B, right). In contrast, intense hRad21 signals were detected in control cells, especially at the interface of sister chromatids within the centromere, as has been previously described (Fig. 2 B, left; Waizenegger et al., 2000).

Next, to study the effects of Vpr expression on the chromatin localization of hRad21 in interphase, MIT-23 cells were immunostained for chromatin-bound hRad21, and hRad21 intensities and the nuclear sizes were analyzed (Fig. S2, A and B). Chromatin-associated hRad21 levels were not reduced in regularly sized Vpr-expressing cells during interphase, though they were greatly reduced in mitotic cells (Fig. S2 A). Interestingly, the cells with larger nuclei had statistically less chromatin-bound hRad21 (Fisher's exact test, P = 0.002; Fig. S2 B, bottom). As this population of cells could be produced via defective chromosome segregation (Figs. 1 E and S1 D), the results suggested that the diminished association of hRad21 to the interphase chromatin was observed after hRad21 mislocalization at mitosis.

Cohesin loading onto the interphase chromatin depends on NIPBL/delangin in human cells (Toyoda and Yanagida, 2006). This encouraged us to examine the involvement of NIPBL/delangin in the Vpr-induced PCS. RNAi depletion of NIPBL caused specific down-regulation of delangin/NIPBL (Fig. S2 C). The introduction of NIPBL RNAi decreased the hRad21 signal during interphase remarkably (Fig. S2 C, bottom right), whereas chromatin-associated hRad21 was observed in control cells (Fig. S2 C, bottom left). Transfection of MIT-23 cells with NIPBL RNAi did not alter the frequency of PCS (Fig. S2 D). In contrast, and in line with a previous study (Kaur et al., 2005), it induced PCS in 8.3% of control cells (Fig. S2 D). These data suggest that NIPBL is not a primary Vpr target and that Vpr-induced PCS results from cohesin defects that first become apparent in mitosis. Therefore, we then focused on the mitotic phenotypes to clarify the mechanisms underlying Vpr-induced PCS.

Vpr causes failure in protecting cohesin on the mitotic chromatin

Next, we addressed whether Vpr-induced mislocalization of hRad21 was a result of the displacement of the guardian protein hSgo1 from the mitotic centromere chromatin. MIT-23 cells and their chromosome spreads were immunostained for hSgo1 (Fig. 2 C). Upon Vpr expression, hSgo1 was undetectable on spread chromosomes and prometaphase cells (Fig. 2 C, bottom

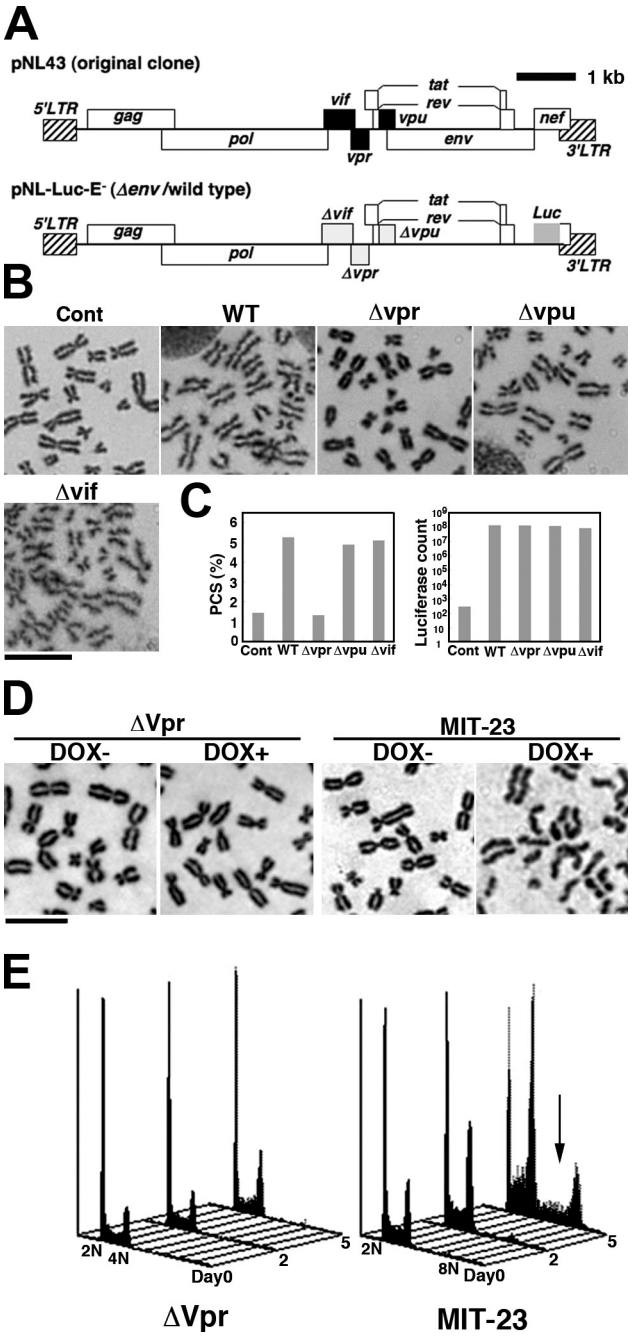

Figure 1. **Vpr mediates HIV-1–induced PCS.** (A) A schematic structure of HIV-1 pNL43 (original clone) and pNL-LUC-E⁻ (*Δenv*/wt). wt and mutant viruses were *env* deficient (*Δenv*), and *nef* was replaced by the *luciferase* (*Luc*) gene. The accessory genes *vif*, *vpr*, and *vpu* were mutated (yielding *Δvif*, *Δvpr*, and *Δvpu*, respectively). (B) Representative chromosome spreads from PBLs infected or not infected with wt or mutant virus (*Δvpr*, *Δvpu*, or *Δvif*). PBLs were synchronized with colcemid. Cont, control. Bar, 10 µm. (C) A luciferase assay was used to determine the virus production rate (right) and PCS frequency (left). (D) Chromosome spreads were Giemsa stained. At 48 h, the frequency of PCS was >40% in DOX-induced Vpr-transfected cells (far right) and <3% in nontreated cells (middle right). In contrast, mock-transfected cells (ΔVpr) showed no difference in PCS frequency with or without DOX treatment (<3%; left). Bar, 5 µm. (E) The cell cycle was analyzed using FACS after DOX addition (days 0–5). ΔVpr (left) and MIT-23 (right) cells are shown. Arrow, hyperploidy/aneuploidy. All data are representative of at least three independent experiments.

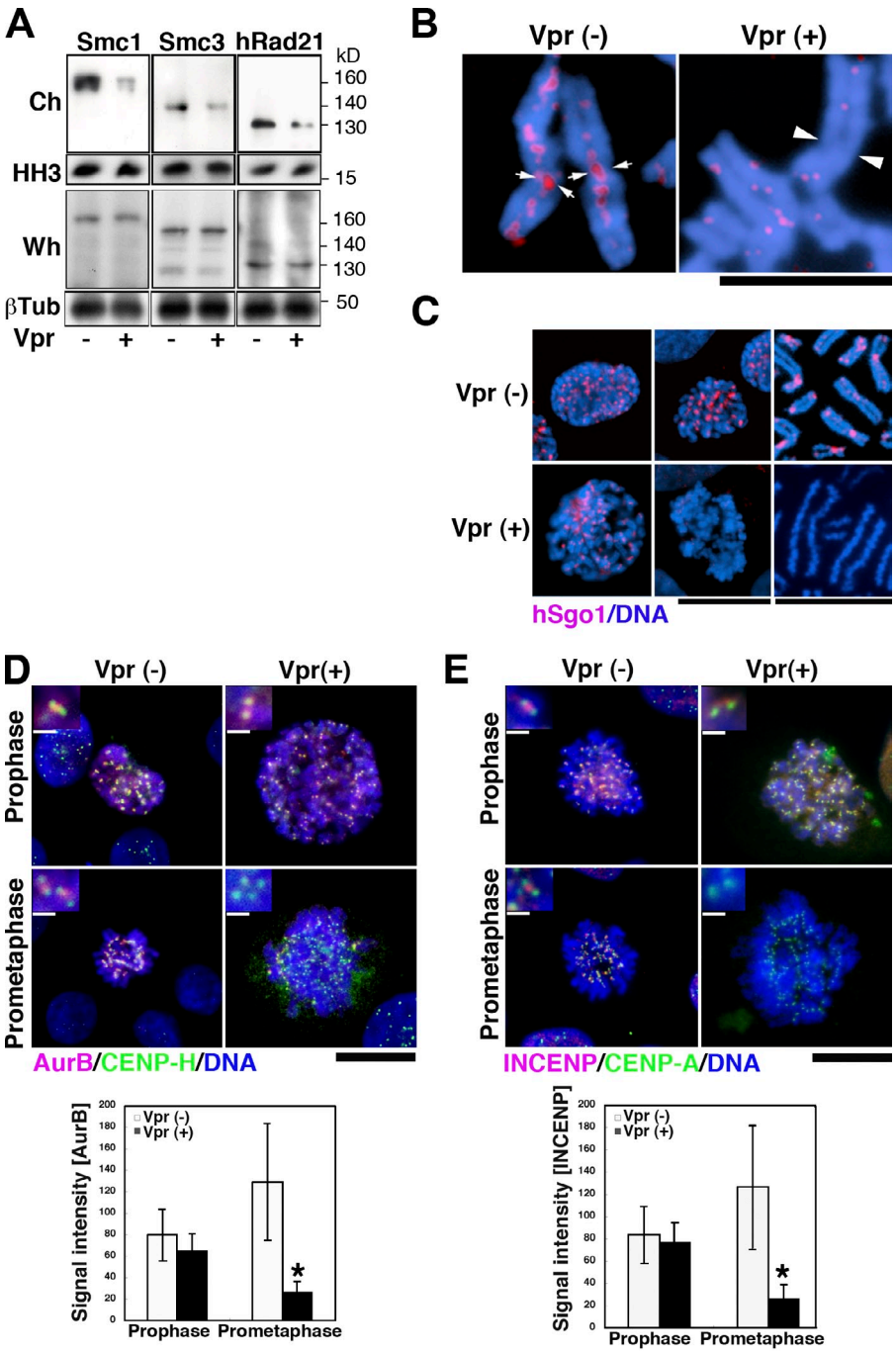

Figure 2. **Altered localization of cohesin and its regulators in Vpr-expressing cells.** (A) Expression of the cohesin proteins Smc1, Smc3, and hRad21 in DOX-treated MIT-23 versus ΔVpr cells at 48 h. Ch, isolated chromatin; Wh, whole-cell lysate. Loading controls: histone H3 (HH3) and β-tubulin (βTub). Data are representative of at least three independent experiments. (B) Anti-hRad21 staining in DOX-treated MIT-23 cells versus ΔVpr cells. Arrows indicate hRad21 signals at the interface of sister chromatids within the centromere, and arrowheads indicate undetectable hRad21 signals at loosely aligned sister chromatids. Blue, DNA; red, hRad21. Similar results were obtained in three independent experiments. (C) Anti-hSgo1 immunostaining. (D and E, top) Immunostaining of AurB (D) or INCENP (E) in early mitosis. (insets) Magnifications of the centromere. (bottom) Intensities of AurB (D) or INCENP (E) at the inner centromere region. *, $P < 0.0001$ (AurB) and $P = 0.0002$ (INCENP) versus Vpr-expressing cells in prophase. Values represent the mean ± SD. (C–E) Results are representative of three independent experiments. Bars: (B and C [right]) 5 µm; (C [middle], D, and E) 10 µm; (D and E, insets) 0.5 µm.

right and middle), but prophase cells exhibited centromere localization of hSgo1 (Fig. 2 C, bottom left). As AurB and inner centromere protein (INCENP), which form a protein complex chromosomal passenger complex (CPC; Adams et al., 2001), regulate hSgo1 localization (Kawashima et al., 2007; Pouwels et al., 2007), their localization was assessed on Vpr expression (Fig. 2, D and E). AurB and INCENP targeting to the inner centromere was reduced significantly in Vpr-expressing prometaphase cells but not in prophase, whereas the centromere localization of CENP-A and CENP-H proteins was not affected ($P < 0.01$; Fig. 2, D and E). These data indicate that Vpr causes failure in the protection of cohesin in mitosis, which becomes apparent after prophase.

Vpr expression displaces HP1 and hMis12 from chromatin

In fission yeast, Swi6, an HP1 homologue, functions as a key regulator of centromere cohesion during mitosis (Nonaka et al., 2002; Pidoux and Allshire, 2004). HP1-α also regulates the localization of hSgo1 (Yamagishi et al., 2008). Therefore, we analyzed HP1 in Vpr-expressing cells. Western blot analysis using antibodies against three subtypes of human HP1 (HP1-α, HP1-β, and HP1γ; Hayakawa et al., 2003) revealed that Vpr decreased the amounts of HP1-α and HP1-γ in the isolated chromatin (see Materials and methods; Remboutsika et al., 1999) by >90 and 20%, respectively (Fig. 3 A). Comparable results were obtained upon immunostaining chromatin-bound HP1-α

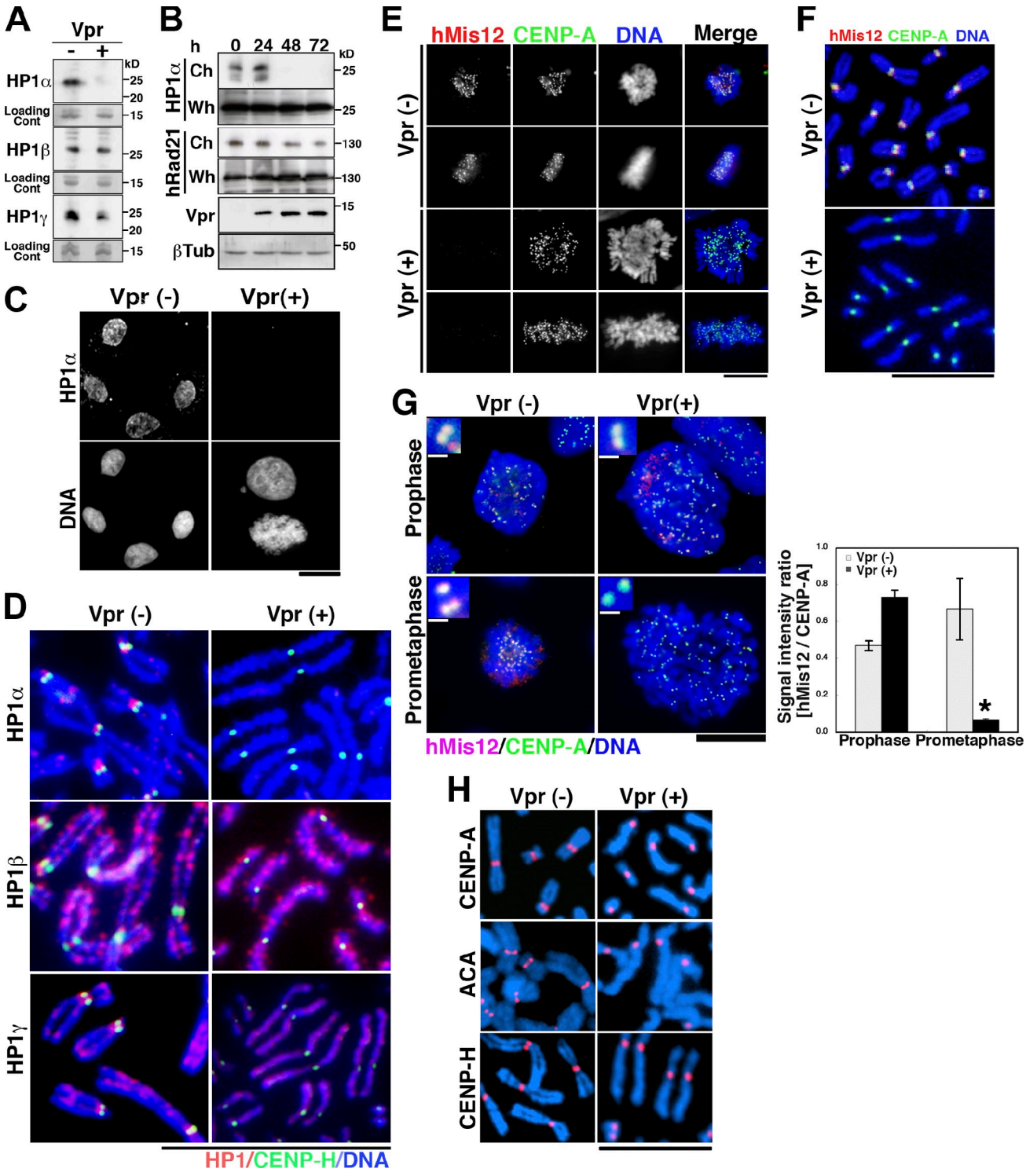

Figure 3. **Altered localization of HP1-α, HP1-γ, and hMis12 proteins in Vpr-expressing cells.** (A) HP1-α, HP1-β, and HP1-γ expression in DOX-treated MIT-23 and ΔVpr cells. Loading control (Cont): a major band of the chromosomal fraction corresponding to 15 kD by Coomassie brilliant blue staining. (B) Chronological changes in HP1-α and hRad21 in the chromosomal (Ch) versus whole-cell (Wh) fractions after DOX addition (days 0–3). βTub, β-tubulin; Vpr, Vpr expression. Data are representative of three independent experiments. (C) Cells were preextracted with PBS containing Triton X-100 and stained with anti–HP1-α antibody and Hoechst 33342. In the bottom right, the pictured cells are in interphase (top cell) and undergoing mitosis (bottom cell). Similar results were obtained in at least three independent experiments. (D) Chromosome spreads were immunostained for HP1 subtypes and CENP-H. Similar results were obtained in three independent experiments. (E) Mitotic cells were immunostained for hMis12 and CENP-A. (F) Chromosome spreads prepared from DOX-induced cells (48 h) were immunostained for hMis12 and CENP-A. (G, left) DOX-induced cells (48 h) were immunostained for hMis12 and CENP-A. (insets) Magnifications of the centromere. (right) The hMis12/CENP-A signal intensity ratio was measured during prophase and prometaphase. Gray bars, ΔVpr cells; black bars, MIT-23 cells. Values represent the mean ± SD (three experiments) of data generated using the cells shown on the left. *, P = 0.0008 versus Vpr-expressing cells in prophase. (H) Chromosome spreads immunostained with CENP-A and CENP-H antibodies and ACA antisera. Blue, DNA; red, CENP-A, ACA, or CENP-H. Vpr (−), DOX-treated ΔVpr cells at 48 h; Vpr (+), DOX-treated MIT-23 cells at 48 h. Bars: (C, E, and G) 10 μm; (D, F, and H) 5 μm; (G, insets) 0.5 μm.

and HP1-γ (Fig. S2 E). In striking contrast, no apparent decrease in HP1-β was detected (Fig. 3 A, middle row). Time course analysis of HP1-α and hRad21 proteins revealed that HP1-α from the isolated chromatin (Remboutsika et al., 1999) was undetectable within 48 h of the induction of Vpr expression (Fig. 3 B, top). The hRad21 levels from the chromatin isolated using a reported protocol (Todorov et al., 1995) also decreased over a 72-h period. In addition, the total amount of each protein in whole-cell extracts remained unchanged when Vpr was expressed (Fig. 3 B), suggesting that Vpr alters their subcellular localization without modulating their overall expression. Next, we characterized the chromatin-associated HP1-α levels immunohistochemically and found that HP1-α became undetectable under Vpr expression within 48 h in both mitotic and interphase cells (Fig. 3 C, top right). In contrast, it was clearly detected in control cells (Fig. 3 C, top left). Notably, chromatin-associated HP1-α loss was observed in most of the Vpr-expressing interphase population (Fig. S2 E). However, the chromatin-associated hRad21 loss was not major in regularly sized nuclei but was observed significantly in large nuclear cells (Fig. S2 B). These observations support the idea that a defect in HP1-α precedes the alteration in hRad21.

To identify which subtypes of HP1 proteins were affected for the chromosome localization by Vpr, we investigated the localization of HP1 during mitosis immunohistochemically (Fig. 3 D). In control cells, HP1-α localized to pericentromere regions and the inner centromere, consistent with a previous study (Kiyomitsu et al., 2010). HP1-β localized to the chromosome arm, and HP1-γ localized to both the chromosome arm and centromeric regions (Fig. 3 D, left). Morphological analysis of chromosome spreads from Vpr-expressing cells detected PCS in those lacking a centromeric HP1-α or HP1-γ signal but not those lacking a HP1-β signal (Fig. 3 D, right). CENP-H, a component of the inner kinetochore, was unaffected in Vpr-expressing cells (Fig. 3 D, right). These data suggest that HP1-α is the HP1 subtype that is most strongly influenced by Vpr expression during mitosis.

HP1-α and HP1-γ physically interact with hMis12, a kinetochore protein essential for chromosome segregation (Goshima et al., 2003; Obuse et al., 2004). Thus, hMis12 targeting in Vpr-expressing cells was analyzed. Immunohistochemical analysis revealed that hMis12 was undetectable at mitotic kinetochores in Vpr-expressing cells. (Fig. 3 E), whereas the centromere-specific histone H3 variant CENP-A was unaffected (Fig. 3 E). Simultaneous morphological analysis of chromosome spreads detected PCS in spreads that lacked hMis12 signals (Fig. 3 F, bottom). In addition, centromere proteins detected by an anti-centromere antibody (ACA) that primarily binds to CENP-B were also unaffected by Vpr, similar to CENP-A and CENP-H (Fig. 3 H, right). We then characterized hMis12 localization during mitosis. In Vpr-expressing cells, hMis12 and CENP-A signals were both detectable at prophase (Fig. 3 G, top right). However, the hMis12 signal became nearly undetectable at prometaphase (Fig. 3 G, bottom right). CENP-A was detected in the same specimens on separated sister chromatids (Fig. 3 G, bottom right inset). To obtain more robust data, the relative signal intensities of hMis12 and CENP-A were measured in >400 sister kinetochores at prophase and prometaphase (see Materials and methods). In Vpr-expressing cells, the hMis12/CENP-A signal ratio was decreased significantly when cells entered prometaphase ($P < 0.01$; Fig. 3 G, black bar), whereas in control cells, it was comparable to that measured at prophase (Fig. 3 G, gray bar). These results suggest that Vpr interferes with the heterochromatin structure by displacing HP1-α/-γ proteins in interphase and that their displacement affects the localization of the centromere chromatin proteins hMis12, hSgo1, and CPC (Fig. 2) after prophase.

HP1-α and HP1-γ are required for chromatid cohesion during mitosis in human cells

In an effort to obtain direct evidence indicating that the altered localization of HP1 is critical to cohesion defects caused by Vpr, the effects of down-regulating HP1-α and HP1-γ on centromere cohesion were investigated. Endogenous expression of HP1-α or HP1-γ was knocked down using RNAi, and specific knockdown was confirmed by immunoblotting (Fig. S3 B). RNAi-treated cells were arrested by nocodazole, and then Giemsa-stained chromosome spreads were examined (Fig. 4 A). Note that chromosomes from HP1-α and HP1-γ (HP1-αγ) RNAi cells appear swollen, with indistinct primary constrictions (Fig. 4 A), consistent with the morphological changes reported in hRad21-depleted cells (Toyoda and Yanagida, 2006). After transfection with HP1-α and HP1-γ siRNA, PCS was induced in 10.7 and 4.2% of cells (Fig. 4 B), respectively. When both HP1-α and HP1-γ were knocked down (HP1-αγ RNAi), PCS occurred more frequently (in 19.8% of the spreads examined).

To provide further evidence that HP1-αγ depletion is linked directly to cohesin loss, we monitored the expression of exogenous myc8-tagged hRad21. HeLa cells were transfected with a plasmid encoding myc8 epitope–tagged hRad21 (phRad21-myc8) with or without HP1-αγ RNAi. Subsequently, we examined the expression of hRad21-myc8 by detecting the myc tag (see Materials and methods). Approximately 70% of cells treated with control siRNA were positive for hRad21-myc8 (myc positive) within the pericentromeres (Fig. 4 C). In contrast, introduction of HP1-αγ RNAi reduced the number of myc-positive cells to 30% (Fig. 4 C). Of note, PCS was observed in myc-negative cells (Fig. 4 D, right), clearly indicating that the down-regulation of HP1-αγ induced cohesin defects that correlated with PCS. Our data support the idea that dissociation of HP1 from the heterochromatin is involved in Vpr-induced PCS. To further characterize Vpr-induced PCS, we transfected cells with hSgo1 RNAi and compared the phenotypic changes in chromosome spreads. Down-regulation of hSgo1 protein was confirmed by immunoblotting (Fig. S3 A). Representative chromosome spreads prepared from Vpr-expressing cells or HP1-αγ RNAi cells are shown in Fig. 4 E, and summarized results are also shown (Fig. 4, F and G). The effects of hSgo1 RNAi on the loss of cohesin caused by the down-regulation of HP1-αγ were monitored using phRad21-myc8. Approximately 30% of the cells were myc negative with control RNAi, and the numbers of myc-negative cells were dramatically increased upon transfection with HP1-αγ RNAi (Fig. 4, H and I).

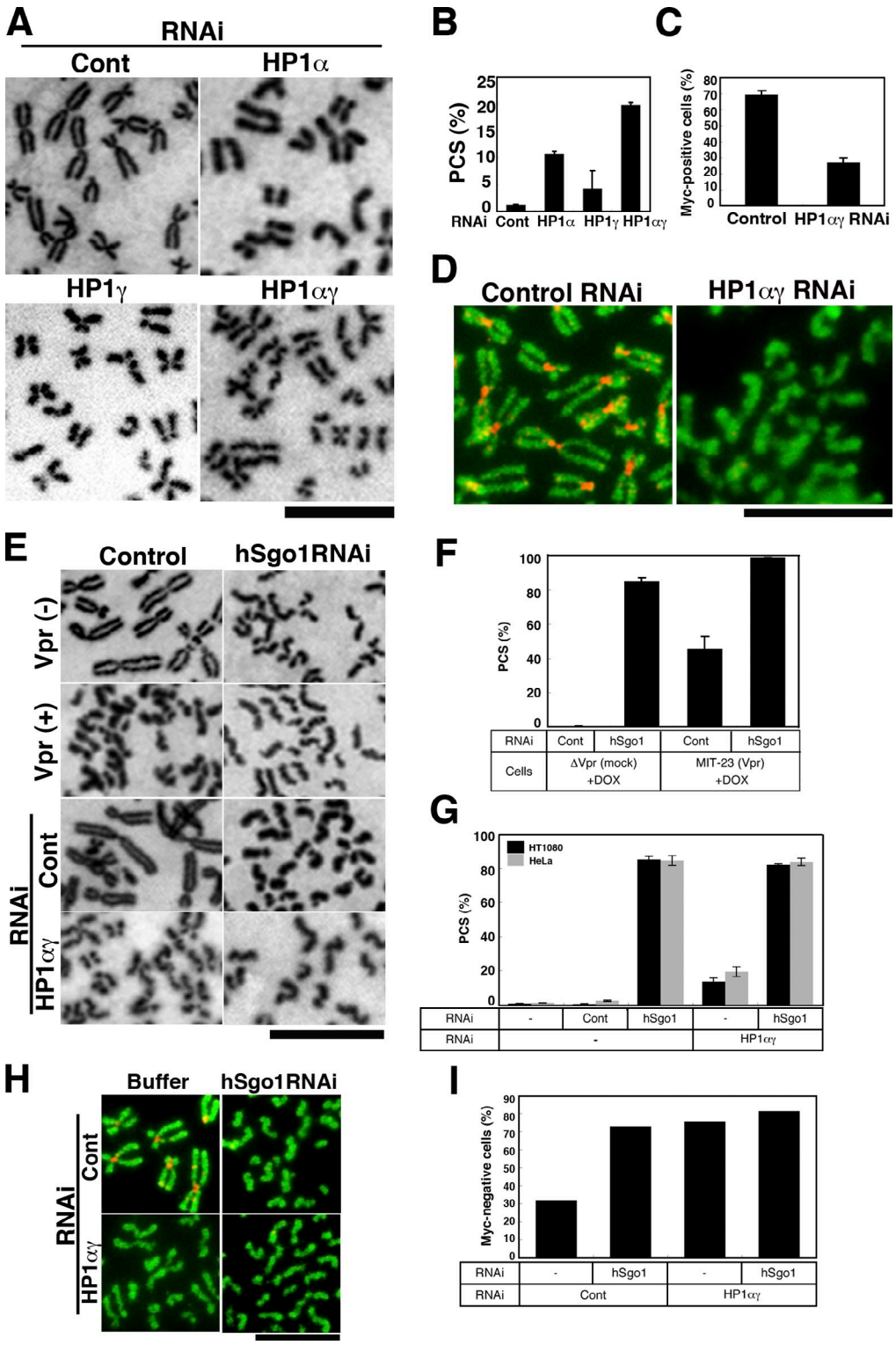

Figure 4. **Loss of cohesin from the mitotic centromere by HP1-αγ RNAi.** (A) Giemsa-stained chromosomes from HeLa cells transfected with control (Cont), HP1-α, HP1-γ, or combined HP1-α + HP1-γ (HP1-αγ) siRNA (48 h). (B) PCS frequencies. (C) Frequency of hRad21-myc8–positive cells among HH2B-EGFP–positive cells transfected with control or HP1-αγ siRNA. (D) Control or HP1-αγ siRNA–transfected HeLa cells were cotransfected with hRad21-myc8 and histone H2B-EGFP (HH2B-EGFP). Chromosome spreads were stained for c-myc (red) and EGFP (green). Similar results were obtained in three independent experiments. (E) Giemsa-stained chromosome spreads from cells transfected with no RNA (control) or with hSgo1 siRNA (48 h). ΔVpr cells + DOX (top), MIT-23 cells + DOX (top middle), HeLa cells and control RNAi (bottom middle), and HeLa cells and HP1-αγ RNAi (bottom) are shown. (F) PCS frequencies in cells transfected with hSgo1 or control siRNA with or without Vpr expression. (G) PCS frequency in HeLa and HT1080 cells transfected with hSgo1 or control siRNA with or without HP1-αγ RNAi. (H and I) Cells were transfected with control or hSgo1 siRNA with or without HP1-αγ RNAi followed by hRad21-myc8 transfection (48 h). (H) Chromosome spreads stained for c-myc (red) and EGFP (green). (I) Frequency of myc-negative cells among HH2B-EGFP–positive cells. (H and I) Similar results were obtained in two independent experiments, and representative data are shown. (B, C, F, and G) Values represent the mean ± SD of three independent experiments. Bars: (A and E) 5 μm; (D and H) 10 μm.

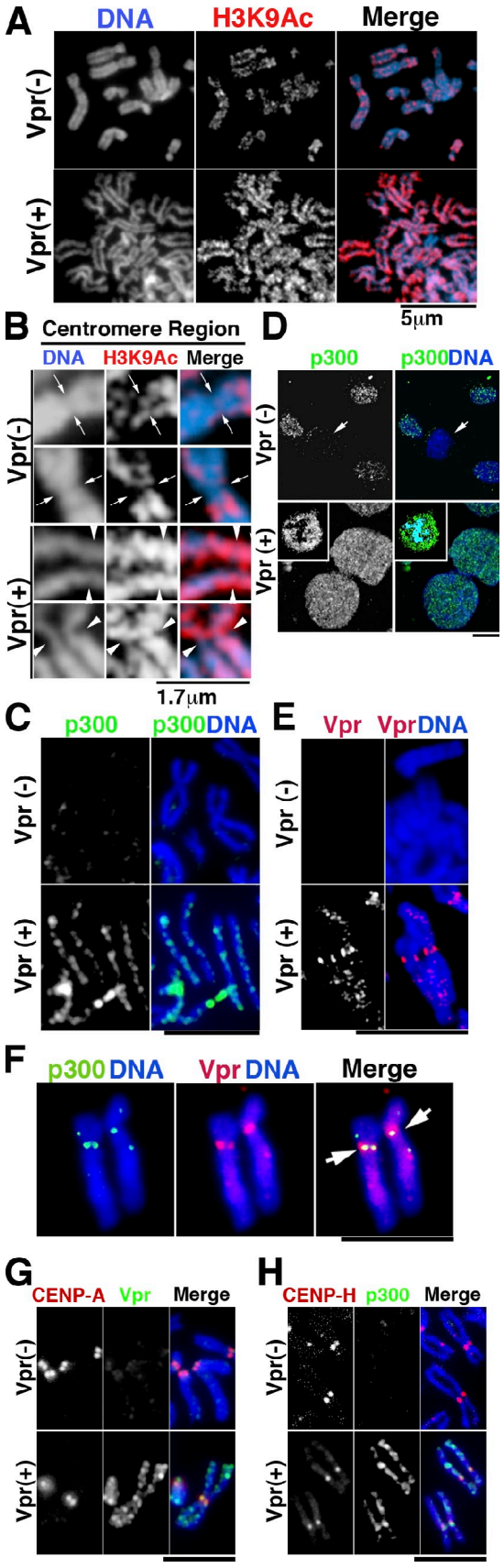

Figure 5. **Forced association of p300 with chromatin in Vpr-expressing cells.** Chromosome spreads were prepared from DOX-treated cells at 48 h. Vpr (−), ΔVpr cells; Vpr (+), MIT-23 cells. (A) Histone H3 lysine 9 is strongly acetylated in the chromosomes, including centromeric regions. Chromosome spreads were immunostained with antiacetylated H3K9 antibody. (B) Typical centromere regions shown at a higher magnification. H3K9 was highly acetylated along the whole chromosome, including the centromere region, in Vpr-expressing cells (arrowheads). However, only a weak signal was detected at the primary constrictions of the chromosomes in control cells (arrows). (C) Chromosome spreads stained for p300. (D) Preextracted cells stained for p300. Arrows, cells undergoing mitosis. Insets, mitotic cells expressing Vpr. ΔVpr cells + DOX (top) and MIT-23 cells + DOX (48 h; bottom) are shown. (E) Chromosome spreads stained for Vpr. (F) Chromosome spreads from DOX-treated MIT-23 cells stained for Vpr and p300. Arrows, signals at the centromere. Two pairs of sister chromatids are shown. (G and H) Chromosome spreads stained for CENP-A and Vpr (G) and CENP-H and p300 (H). Similar results were obtained in three independent experiments. Bars: (C and E–H) 5 μm; (D) 10 μm.

hSgo1 RNAi increased PCS under any of the tested conditions (Fig. 4 G) and produced a remarkable increase in the myc-negative cell population (Fig. 4, H and I), suggesting that hSgo1 acts downstream of HP1-αγ in the maintenance of centromeric cohesin during mitosis. These observations were similar to those for Vpr-induced PCS (Fig. 4 F), lending support to the notion that Vpr-induced PCS depends on the disruption of HP1-αγ function.

Chromatin recruitment of p300 by Vpr and displacement of HP1 from chromatin

Given that Vpr interacts directly with p300/HAT (Kino et al., 2002), a HAT-regulating transcription (Boyes et al., 1998; Caron et al., 2003), and that HP1-α binds chromatin via histone H3 methylated at lysine 9 (H3K9; Jenuwein and Allis, 2001), we tested whether Vpr alters HP1-α localization by modifying the properties of this histone. First, we attempted to detect the acetylated form of H3K9 in condensed chromosomes, as Vpr-induced cohesin defects were specifically induced during mitosis. H3K9 associated with condensed chromosomes prepared from Vpr-expressing cells was highly acetylated (Fig. 5 A, bottom middle). Note that acetylated H3K9 was detected at sites of primary chromosome constriction (Fig. 5 B, bottom). In contrast, less acetylated H3K9 was detected at primary constriction sites in control cells (Fig. 5 B, top). Conversely, dimethylation on H3K9 decreased on mitotic chromosomes from Vpr-expressing cells (Fig. S5 A, bottom). Next, we examined p300 localization upon Vpr induction. Interestingly, we detected p300 in the condensed chromosomes of Vpr-expressing cells (Fig. 5 C, bottom). In marked contrast, p300 signals were not detected in control cells (Fig. 5 C, top). Furthermore, increased levels of chromatin-associated p300 were detected in interphase and mitotic Vpr-expressing cells (Fig. 5 D, bottom insets), whereas no signal was detected in control mitotic cells (Fig. 5 D, top). A detailed analysis of condensed chromosomes showed that the Vpr signal was localized to the chromosome arms and enriched at the primary constriction of chromosomes (Fig. 5 E). Moreover, simultaneous staining showed that p300 and Vpr colocalized on the chromosome (Fig. 5 F, right). Costaining with CENP-A or CENP-H showed that Vpr and p300 localized to the centromere and arm region (Fig. 5, G and H). These data suggest that Vpr actively mobilizes p300 to a range of chromatin regions including the centromeres, resulting in the displacement of HP1-α and PCS.

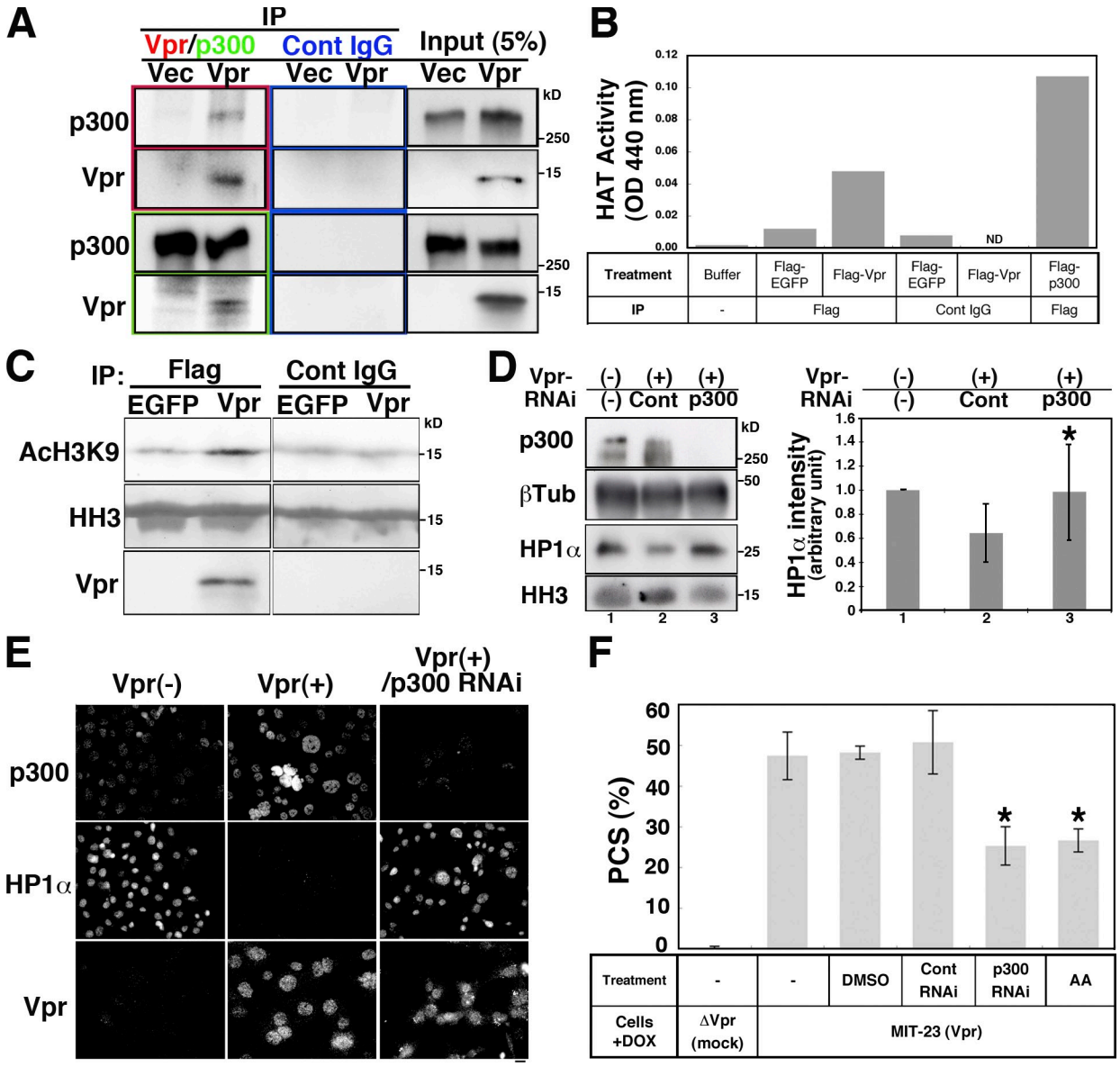

Figure 6. **p300 is required for Vpr-induced PCS.** (A) Expression of p300 or Vpr in immunoprecipitates (IP) measured using anti-Vpr and anti-p300 antibodies and control (Cont) IgG. Cells were transfected with pCMV-Vpr (Vpr) or control vector (Vec). (B) Vpr immunocomplexes exhibit HAT. 293T cells were transfected with Flag-EGFP, Flag-Vpr, and Flag-p300 (positive control), and HAT activity was measured. Flag-immunoprecipitated Flag-Vpr showed higher HAT activity than did Flag-EGFP, control IgG, IP-Flag-EGFP, or Flag-Vpr. IP-Flag-p300 reached maximal levels 2 h before measurement, indicating that actual p300 HAT activity may be higher than the measured value. Results shown are representative of two independent experiments. (C) HAT activity in Vpr-expressing cells. HAT activity targeting histone H3K9 in Flag-EGFP or Flag-Vpr immunoprecipitates was examined using histone H3 (HH3) as a substrate. (D) Expression of HP1-α in the isolated chromatin of Vpr-expressing MIT-23 cells (+DOX, 48 h) transfected with control or p300 siRNA. (left) Immunoblotting of the indicated proteins. β-Tubulin (βTub), whole-cell lysate loading control; HH3, isolated chromatin loading control. (right) Quantification of the HP1-α intensities shown in the immunoblot. RNAi of p300 in Vpr-expressing cells (lane 3) reversed the amount of chromatin-bound HP1-α compared with control RNAi (lane 2) with statistical significance (*, P = 0.046). Values represent the mean ± SD of three independent experiments. (E) Immunostaining of chromatin-bound HP1-α, p300, and Vpr. Typical micrographs are shown. The levels of chromatin-bound HP1-α in Vpr-expressing cells were restored when p300 was down-regulated (right panels). Vpr (−), DOX-treated ΔVpr cells at 48 h; Vpr (+), DOX-treated MIT-23 cells at 48 h. Bar, 10 μm. (F) PCS frequencies in cells treated with p300 siRNA or AA (7.5 μM in DMSO) in the presence of Vpr expression. Values represent the mean ± SD of three independent experiments. *, P = 0.0009 for p300 RNAi and P = 0.0088 for AA versus control RNAi in DOX-induced MIT-23 cells.

p300/HAT is required for Vpr-induced displacement of HP1-α and PCS

To demonstrate the involvement of p300/HAT in Vpr-induced PCS, we further characterized p300 in Vpr-expressing cells. After first confirming that Vpr associated with p300 (Fig. 6 A), we subsequently showed that a Vpr immunoprecipitate demonstrated HAT activity against H3K9 (Fig. 6, B and C). This activity was partially inhibited by anacardic acid (AA), a p300/HAT inhibitor (Fig. S5 B), indicating that p300/HAT was present in the immunoprecipitate, although we cannot exclude a possibility of other HAT contamination in the Vpr immunoprecipitate.

Intriguingly, a Western blot analysis revealed that p300 RNAi restored chromatin retention of HP1-α in cells expressing Vpr (Fig. 6 D). Immunohistochemical analysis revealed

that p300 RNAi restored the chromatin levels of HP1-α in Vpr-expressing cells (Figs. 6 E and S4, A [right] and B). RNAi depletion of p300 specifically down-regulated the p300 levels (Figs. 6 E, S3 A, and S4 A [left]). These data strongly suggest that p300 was responsible for the displacement of HP1-α from chromatin.

To provide more convincing evidence that HAT/p300 contributes to Vpr-induced PCS, we performed additional experiments. First, we showed that AA reduced the rate of PCS (Fig. 6 F). Importantly, we confirmed that AA did not inhibit the chromatin recruitment of p300 in Vpr-expressing cells (Fig. S5, C and D). Second, we demonstrated that the down-regulation of p300 using RNAi also reduced the frequency of Vpr-induced PCS (Fig. 6 F). Moreover, although forced expression of p300 cDNA increased the frequency of Vpr-induced PCS (Fig. 7, A–C), neither PCS nor an increase in the level of chromatin-associated p300 was observed in the absence of Vpr expression (Figs. 7 [C–E] and S4). Forced expression of p300 cDNA lacking a catalytic domain (amino acids 1,472–1,522; *ΔHAT-p300*; Fig. 7 A) did not increase the frequency of Vpr-induced PCS (Fig. 7 C). We confirmed this finding through back transfection with an expression plasmid encoding an RNAi-resistant wt p300 cDNA (Fig. 7 F). Transfection with this plasmid increased the rate of Vpr-induced PCS, reversing the effects of p300 RNAi (Fig. 7, F–H). In contrast, a second plasmid encoding an RNAi-resistant form of *ΔHAT-p300* did not affect the rate of PCS ($P < 0.01$; Fig. 7 H). We confirmed that both plasmids fostered similar levels of p300 expression (Fig. 7 G), with p300 being associated with chromatin in Vpr-expressing cells (Fig. 7, D and E). These data led us to conclude that the catalytic activity of p300 is crucial to Vpr-induced PCS and that Vpr aberrantly recruits p300 to chromatin, causing HP1-α to be displaced.

Discussion

HIV-1 infection has come to be considered a chronic infection since the introduction of antiretroviral therapy, which can be used to control HIV-1 production for extended periods, thereby improving patient prognosis (Mermin et al., 2008). However, integrated HIV-1 proviral copies cannot be eradicated from the host genome, and small numbers of progeny virions are still produced during therapy (Corbeau and Reynes, 2011). Therefore, it is essential to know how the virus influences host cells. Previously, we detected ∼10 ng/ml Vpr in HIV-1–infected patient sera (Hoshino et al., 2007), and we showed that Vpr-expressing cells exhibited hyperploidy and aneuploidy (Shimura et al., 1999). We also found PCS, a hallmark of aneuploidy (Thompson et al., 1993; Kajii et al., 2001), in HIV-1–infected individuals (Shimura et al., 2005). In this study, we found that the *vpr* gene is responsible for HIV-1–associated PCS. Therefore, we focused on the molecular mechanisms of Vpr-induced PCS.

Vpr-expressing cells induce PCS, which is associated with reduced levels of cohesin, hSgo1, and HP1 and of the related proteins hMis12, AurB, and INCENP at chromatin. Among these proteins, immunofluorescence analyses indicated that HP1-α was mislocalized from insoluble nuclei first, whereas chromatin-bound hRad21 was likely diminished second, suggesting that HP1-α is a key factor in Vpr-induced PCS and that HP1 is essential for centromere cohesion during mitosis in human cells. Vpr displaced HP1, whose RNAi-mediated down-regulation induced PCS concomitant with the displacement of hRad21, consistent with a previous finding for hSgo1 (Yamagishi et al., 2008). Although the functional link between heterochromatin and centromere cohesion in humans remains controversial, Yamagishi et al. (2008) and our current observations suggest a strong functional connection between heterochromatin and centromere cohesion. We further suggest that pathogenic microorganisms can epigenetically impair the function of centromeric heterochromatin.

The present data support the idea that HP1-α plays a major role in centromere cohesion during mitosis and that centromere cohesion may be maintained by a network involving HP1-α and HP1-γ (Obuse et al., 2004). Consistent with our data, immunohistochemical analyses of metaphase spreads have shown that HP1-α associates with centromeres during mitosis (Minc et al., 1999; Hayakawa et al., 2003; Yamagishi et al., 2008; Kiyomitsu et al., 2010). On the other hand, all subtypes of HP1 are released from chromatin during M phase as a result of histone H3 phosphorylation, which is mediated by AurB kinase (Fischle et al., 2005; Hirota et al., 2005). These findings suggest that most HP1 proteins are released during mitosis but that a small amount of HP1-α remains in the centromere region with hSgo1 to protect cohesin from removal until the onset of anaphase.

Notably, our observation suggests that the HP1-αγ–mediated regulation of cohesion is especially important during mitosis. Accordingly, AurB, INCENP, hSgo1, and human inner kinetochore protein (hMis12) were initially observed during prophase at the centromere, even in cells in which HP1-αγ was down-regulated by Vpr, but these proteins were displaced when the cells entered prometaphase. Given that the depletion of AurB or INCENP by RNAi resulted in altered hSgo1 localization during mitosis, whereas hSgo1 RNAi did not significantly affect AurB or INCENP localization to the inner centromeres (Kawashima et al., 2007; Pouwels et al., 2007), the effect of the loss of hSgo1 on Vpr expression may be mediated by the loss of the CPC from the inner centromere. These observations further suggest that cohesion is maintained by a network involving HP1-α and HP1-γ, especially during mitosis.

In Vpr-induced PCS, p300 might be responsible for the displacement of HP1-α from chromatin. In particular, the interaction of Vpr and p300 is essential for the displacement of HP1-α from chromatin, as mutant Vpr with a defective p300-binding leucine/arginine-rich (LR) domain (LR mutant; Kino et al., 2002) caused no apparent induction of PCS (Fig. S5 E). In our study, the artificial expression of p300 by itself resulted in neither the localization of p300 at insoluble nuclei nor PCS. In control cells, no association with p300 was detected in chromosome spreads, although an appropriate amount of p300 is essential for proper chromosome segregation (Ha et al., 2009). These data suggest that the stabilized association of p300 with chromatin as seen in Vpr-expressing cells is unusual. Interestingly, the abnormal association of p300 with chromatin through

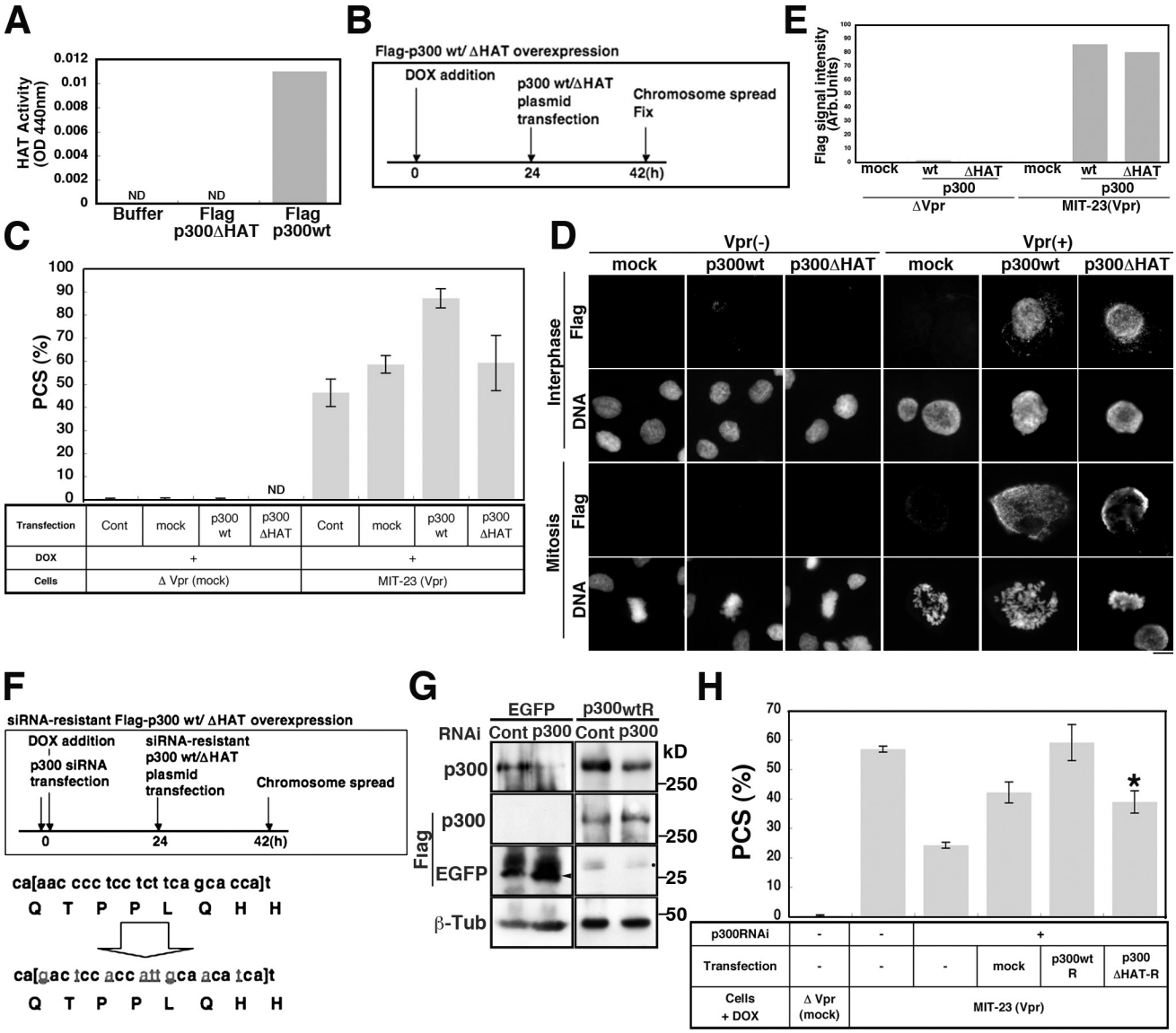

Figure 7. **p300 HAT activity is required for Vpr-induced PCS.** (A) HAT activity in Flag-p300– or Flag-p300ΔHAT–expressing cells. The acetyltransferase deletion mutant p300ΔHAT (Δ1,472–1,522) displayed no activity in a HAT activity assay. Mean values are shown. ND, none detected. Results shown are representative of two independent experiments. (B) A schematized experimental procedure of C. (C) PCS frequency in Vpr-expressing and -nonexpressing cells transfected with pFlag-p300 or pFlag-p300ΔHAT (48 h). Values represent the mean ± SD for independent experiments (n = ∼2–8). Cont, control. (D) The chromatin loading of Flag-p300 or Flag-p300ΔHAT protein in cells expressing Vpr. Cells were preextracted with PBS containing Triton X-100 and stained for Flag M2 epitope and DNA. Levels of chromatin-bound Flag-p300 or Flag-p300ΔHAT were comparable in Vpr-expressing cells. Non–Vpr-expressing cells contained no chromatin-bound Flag-p300 or Flag-p300ΔHAT. Bar, 10 µm. (E) Quantification of Flag-p300/Flag-p300ΔHAT signal intensities in D. Results shown are representative of two independent experiments. Arb., arbitrary. (F, top) A schematized experimental procedure of G and H. Gray underlined letters represent mutation sites in the RNAi-resistant wt and p300ΔHAT cDNA plasmids. (bottom) Mutations introduced to prepare RNAi-resistant Flag-p300wt (pFlag-p300wtR) and RNAi-resistant p300ΔHAT (p300ΔHAT-R). (G) Western blotting to verify that the expression of pFlag-p300wtR was not affected by p300RNAi. Arrowhead, Flag-EGFP; dot, nonspecific band. βTub, β-tubulin. (H) PCS frequency in Vpr-expressing cells transfected with pFlag-p300wtR or p300ΔHAT-R (48 h) and plasmids carrying RNAi-resistant Flag-p300wt and RNAi-resistant p300ΔHAT. Values represent the mean ± SD of three independent experiments. PCS frequency was significantly lower in cells expressing p300ΔHAT-R than in those expressing p300wtR. *, P = 0.0003.

Vpr was found both in interphase and M phase. The Vpr-mediated binding of p300 to chromatin could be essential for the displacement of HP1-α. However, the molecules required for the chromatin recruitment of Vpr remain to be clarified.

A variety of microorganisms expresses proteins that target p300/HAT and modulate its activity (Hottiger and Nabel, 2000; Caron et al., 2003). p300 functions as a critical regulator of transcription from integrated HIV-1 long terminal repeats (LTRs; Marzio et al., 1998). Vpr, meanwhile, has been shown to cooperate with p300 and to enhance the transcriptional activity of LTRs by up-regulating NF-κB (Felzien et al., 1998). Our results suggest that the enhanced LTR transcription may be mediated by Vpr-induced p300 retention as a result of binding to chromatin. Host cells suppress HIV-1 LTR activity by histone deacetylation, as HIV-1 enters latency through histone deacetylase (HDAC) recruitment to HIV-1 LTRs (Williams et al., 2006), and HDAC inhibitors increase HIV-1 expression (Matalon et al., 2011). HAT activity caused by the p300–Vpr

complex at chromatin may contribute to viral transcription by overcoming host cell HDACs. Moreover, Vpr-mediated p300 binding to chromatin may provide an advantage for viral integration. It is notable that integration of the HIV-1 genome into that of the host cell occurs preferentially near transcriptionally active genes (Brady et al., 2009). The Vpr-induced association of p300 with chromatin may influence transcriptional activity and hence favor viral integration. Cereseto et al. (2005) reported that the HIV-1 protein integrase, which catalyzes HIV-1 integration (Chow et al., 1992), bound p300 directly and that the acetylated integrase showed increased affinity for DNA and stimulated viral integration. The stabilized association of p300 with chromatin caused by Vpr may facilitate the active recruitment of integrase to chromatin, thereby favoring efficient integration of the viral genome. We anticipate that the Vpr-induced stable association of p300 with chromatin may favor active viral production by affecting the functions of other nuclear proteins. It was recently proposed that p300/HAT antagonists could be useful in anti-AIDS therapies (Mantelingu et al., 2007). Blocking the molecular interactions of Vpr and p300 could inhibit the recruitment of p300/HAT to chromatin and thus reduce viral replication. It could also reduce the genomic instability associated with PCS.

This is the first study to reveal centromere cohesion impairment via the epigenetic disruption of heterochromatin by a viral pathogen. The use of Vpr expression, RNAi, and specific inhibitors, in combination with appropriate functional assessments, revealed a new specific mechanism of chromosome cohesion. Vpr expression could therefore be considered a useful system for further study of the complex regulation of chromatin dynamics.

Materials and methods

Viruses and infection

VSV-G–pseudotyped viruses were produced by cotransfecting 293T cells with the infectious HIV-1 proviral clones pNL-Luc-E$^-$ (wt; Connor et al., 1995), pNL-Luc-E$^-$F$^-$ (Vif deficient; Kinomoto et al., 2007), pNL-Luc-E$^-$R$^-$ (Vpr deficient; Connor et al., 1995), and pNL-Luc-E$^-$U$^-$ (Vpu deficient; Iwabu et al., 2009) using the VSV-G expression vector pHIT/G (Fouchier et al., 1997) and FuGENE 6 transfection reagent (Roche). Levels of p24 antigen in culture supernatants were measured using an HIV-1 p24 antigen capture ELISA kit (ZeptoMetrix). PBLs were donated by healthy volunteers approved by the Institutional Ethics Committee of the National Center for Global Health and Medicine. 1.5×10^6 PBLs were infected with 2 ng/ml p24 antigen from wt or mutant virus (multiplicity of infection 0.007) to obtain a similar PCS frequency to that typically found in HIV-1 patients (Shimura et al., 2005) in the presence of 2% phytohemagglutinin-M form (Invitrogen). 82 h later, infected cells were analyzed for luciferase activity using PicaGene (Toyo Ink) and for overall protein content using a bicinchoninic acid assay (Thermo Fisher Scientific). Luciferase counts were normalized using the total protein in infected cells.

Cells

The cell lines used in this study were HT1080, a human fibrosarcoma cell line (JCR B9113; Health Science Research Resource Bank); MIT-23, a DOX-inducible Vpr-expressing cell line (Shimura et al., 1999); ΔVpr mock-transfected cells derived from HT1080 cells; 293T cells; and HeLa cells. All cell lines were cultured in a humidified incubator in DME (Nissui) supplemented with 10% FBS at 37°C and in a 5% CO_2 atmosphere. To induce Vpr expression in MIT-23 cells, 3 µg/ml DOX (Sigma-Aldrich) was added to the culture medium. Vpr protein expression was detected within 24 h of DOX treatment. More than 95% of the DOX-treated cells expressed Vpr, as confirmed by immunostaining. At 48 h after treatment, the mitotic index in DOX-induced MIT-23 cells had increased by ∼8%, whereas it had increased by <2% in noninduced ΔVpr control cells.

DNA plasmids and transfection

A plasmid encoding hRad21-myc8 (phRad21-myc8) was constructed by inserting the entire coding region of hRad21 and eight tandem copies of the myc antigen in-frame into pcDNA3.1/V5His6 (Invitrogen), as previously described (Toyoda and Yanagida, 2006). The plasmid pH2BGFP encodes the chimeric protein histone H2B-EGFP (Kanda et al., 1998). The phRad21-myc8 and pH2BGFP plasmids were cotransfected into HeLa cells at a 5:1 ratio using the Effectene Transfection kit (QIAGEN). A DNA plasmid encoding Flag-tagged wt p300 (pFlag-p300wt) was generated using pFlag-p300ΔHAT, together with Flag and p300wt, as previously described (Boyes et al., 1998). The 5′ fragment of pFlag-p300ΔHAT was excised using SnaBI and XbaI, recovered, and ligated into the corresponding p300wt sites. To generate DNA expression plasmids encoding an siRNA-resistant form of p300, a 2.5-kb SpeI fragment (nucleotides 420–2,870 from the initiation codon) was first subcloned into a pBluescript KS II(+) vector (Agilent Technologies). An oligonucleotide cassette (5′-CCAGATGAGCATGGCCCAGCCCCCTATTGTACCCCGGCA[GACTCCACCATTGCAACATCA]TGGACAGTTGGCTCAACCTGGAGCT-3′; brackets identify the siRNA target site, whereas underlined nucleotides are mismatched but encode the same amino acids) was inserted between the MscI and SacI sites of p300 cDNA. The sequence of the resulting construct was confirmed by sequencing, and the 2.5-kb SpeI fragment was then excised and inserted into the same sites in pFlag-p300wt and pFlag-p300ΔHAT. The correct orientation of the inserted fragment and the presence of mismatched nucleotides were confirmed by restriction mapping and sequencing, respectively. The primer used to confirm the presence of mismatched nucleotides was 5′-CGGAGCCAAAGGGATATTTG-3′, which is a reverse primer and adheres from nucleotide 2,333 of the p300 cDNA transcription initiation site. A DNA plasmid encoding Flag-tagged EGFP was constructed by inserting an oligonucleotide (5′-AATTACCATGGACTACAAAGACGATGACGACAAG-3′) between the EcoRI and BamHI sites of pBOS2EGFP. Correct oligonucleotide insertion was confirmed by sequencing.

RNAi

siRNAs were used to block the expression of NIPBL, hSgo1, HP1-α, HP1-γ, and p300. The siRNA sequences used are as follows: NIPBL, 5′-GCUUUUGAAUCCUCUAGGATT-3′ (Toyoda and Yanagida, 2006); hSgo1, 5′-CAGUAGAACCUGCUCAGAA-3′ (McGuinness et al., 2005); HP1-α, 5′-CCUGAGAAAAACUUGGAUUTT-3′; HP1-γ, 5′-UAUUUCCUGAAGUGGAAGGTT-3′ (Obuse et al., 2004); and p300, 5′-AACCCCUCCUCUUCAGCACCA-3′ (Debes et al., 2002). A double-stranded RNA with the sequence 5′-UAAGGCUAUGAAGAGAUAC-3′ (siCONTROL nontargeting siRNA #2; Thermo Fisher Scientific) was used as a control. RNAi procedures were performed according to the instructions included in the Oligofectamine kit (Invitrogen) for HeLa cells and the Nucleofector kit T (Lonza) or GenePORTER kit (Genlantis) for HT1080-based cell lines. In single transfections, siRNA was used at a concentration of 200 nM; in combined RNAi treatments, each siRNA was used at a concentration of 100 nM.

FACS analysis

A flow cytometer (FACSCalibur; BD) was used in cell cycle analyses, as previously described (Shimura et al., 1999). In brief, cells fixed in 70% ethanol at −20°C for at least 1 h were treated with 100 µg/ml RNase (Sigma-Aldrich) and stained with 5 µg/ml propidium iodide (Sigma-Aldrich) to allow visualization of the DNA.

Cell extraction and immunoblotting

Chromatin was isolated for HP1 immunoblotting using a combination of previously described methods (Remboutsika et al., 1999). In brief, cells were washed twice in ice-cold PBS and then resuspended in buffer N (15 mM Tris-HCl, pH 7.5, 60 mM KCl, 15 mM NaCl, 5 mM $MgCl_2$, 1 mM $CaCl_2$, 1 mM dithiothreitol, 2 mM sodium vanadate, 250 mM sucrose, protease inhibitor cocktail [Sigma-Aldrich], and 1 mM PMSF). An equal volume of buffer N containing 0.6% NP-40 was then added to the resuspended cells, and the resulting suspension was mixed gently and incubated on ice for 5 min. Nuclei were pelleted by centrifugation at 2,000 *g* for 5 min at 4°C. After three washes in buffer N, they were lysed in 10 mM Pipes buffer, pH 6.5, containing 10 mM EDTA, protease inhibitor cocktail, and 1 mM PMSF. The resulting chromatin pellets were washed once in Pipes buffer and resuspended in SDS-PAGE loading buffer after centrifugation at 6,000 *g* for 10 min at 4°C. Equivalent samples (in terms of initial DNA and the final protein) from the supernatant fractions were subjected to 10–15% SDS-PAGE. A control (β-tubulin, PSTAIRE, HH3, or Coomassie brilliant blue stain) was used to confirm equivalent loadings

in each lane. Cellular extraction for cohesion analyses was performed as previously described (Todorov et al., 1995), with slight modifications. After washing in PBS and cytoskeleton (CSK) buffer (10 mM Pipes, pH 7.0, 100 mM NaCl, 300 mM sucrose, and 3 mM $MgCl_2$), cells were incubated for 5 min at RT in CSK extraction buffer (CSK buffer containing 0.5% Triton X-100, 0.5 mM PMSF, and protease inhibitor cocktail). Particulates were pelleted by centrifugation at 700 *g* for 5 min at 4°C. The resulting pellets were washed three times in CSK extraction buffer and lysed in radioimmunoprecipitation assay buffer (50 mM Tris-HCl, pH 8.0, 150 mM NaCl, 1% NP-40, 0.5% sodium deoxycholate, 0.1% SDS, and protease inhibitor cocktail) and were then sonicated on ice. Equivalent amounts of protein were subjected to 10–15% gradient SDS-PAGE. In immunoblot analysis, cell extracts were transferred to nitrocellulose membranes after SDS-PAGE. After blocking in 10% BSA (Sigma-Aldrich), membranes were incubated with antibodies against SMC1 or SMC3 (provided by K. Kimura, Tsukuba University, Tsukuba, Japan), HP1-α (Millipore), HP1-β or HP1-γ (provided by T. Haraguchi and T. Hayakawa, Kobe Advanced Information and Communications Technology Research Center; National Institute of Information and Communications Technology, Kobe, Japan), NIPBL/delangin (Toyoda and Yanagida, 2006), p300 (Millipore), hRad21 (Abcam), or β-tubulin (Millipore). The anti-Vpr antibody 8D1 (IgG2a) was raised by immunization with a full-length Vpr peptide (Peptide Institute, Inc.; Nakai-Murakami et al., 2007). Immune complexes were detected using anti–rabbit or –mouse IgG Fab fragments (GE Healthcare) conjugated to HRP. Bound antibody was visualized using a Western blot detection system (ECL Plus; GE Healthcare). The intensity of the scanned blots was measured on ImageJ software (National Institutes of Health).

Immunofluorescence microscopy

Immunofluorescence staining was performed as previously described (Shimura et al., 1999). In brief, cells were washed in PBS, fixed in 2% PFA in PBS for 10 min, permeabilized with 0.2% Triton X-100 in PBS for 10 min, and blocked with 10% goat serum or 1% BSA in PBS. To remove soluble proteins while leaving chromatin-bound proteins intact, cells were incubated in PBS or CSK buffer containing 0.2% Triton X-100 and 1% BSA for 5 min on ice and were then fixed in 2% PFA in PBS for 10 min. Primary antibodies against hMis12 (1:1,000; Goshima et al., 2003), AurB (1:200; BD), INCENP (1:200; Bethyl Laboratories, Inc.), CENP-A (1:200; Abcam), CENP-H (1:200; provided by K. Yoda), hRad21 (1:50; Toyoda and Yanagida, 2006), hSgo1 (1:1,000; provided by Y. Watanabe, Tokyo University, Tokyo, Japan), HP1-α (1:100; D15; Santa Cruz Biotechnology, Inc.), p300 (1:100; rabbit pAb N-15; Santa Cruz Biotechnology, Inc.), Vpr (1:400; mouse mAb 8D1), and Flag M2 (1:500; mouse mAb; Sigma-Aldrich) were then applied. Slides were mounted in antifade mounting medium (Kirkegaard and Perry Laboratories) and observed under a microscope (BX50; Olympus) equipped with a Plan Apochromat objective lens with immersion oil (*nd* = 1.516 at 23°C; Olympus) and a charge-coupled device camera (Sensys; Photometrics). Images were acquired using IPLab Spectrum software (Scanalytics, Inc.). TIFF images acquired using IPLab Spectrum were imported into Photoshop (Adobe). Signal intensities per unit area in TIFF images acquired using IPLab Spectrum were measured using ImageJ software. Over 100 sister kinetochores (for hMis12) or inner centromeres (for AurB and INCENP) at prophase and prometaphase were measured.

Preparation of chromosome spreads

Cells were treated with 0.1 µg/ml colcemid (Invitrogen) for 2 h or with 0.1 µg/ml nocodazole (Sigma-Aldrich) for 4 h at 37°C. Rounded cells and cells in mitotic arrest were collected, washed in PBS, and incubated in 75 mM KCl for 10 min at RT. Next, 10% (volume/volume) KCl in freshly prepared Carnoy's solution (a 3:1 mixture of methanol and glacial acetic acid) was added to the cell suspensions, which were then mixed gently. The Carnoy's solution was replaced three times. Drops of cell suspension were then spotted onto glass slides and air dried. To visualize chromosomes, the slides were stained for 5 min with 6% Giemsa (Merck) in phosphate buffer, pH 6.8. More than 300 chromosome spreads were examined in each experiment. A chromosome spread was considered PCS positive if more than three chromosomes lacked linkages between sister chromatids.

Immunofluorescence labeling of chromosome spreads

Immunofluorescence labeling of chromosome spreads was performed as previously described (Jeppesen et al., 1992; Vagnarelli and Earnshaw, 2001), with slight modification. Round cells undergoing mitosis were collected, washed in PBS, gently resuspended in 75 mM KCl, and incubated for 10 min at RT. They were transferred to slides through rotation at 600 rpm for 5 min in a cytocentrifuge (Thermo Fisher Scientific). The margins of the resulting preparations were marked using a PAP Pen (Invitrogen), and the slides were then washed for at least 10 min in buffer A (10 mM Tris-HCl, pH 8.0, 120 mM NaCl, 0.5 mM EDTA, and 0.1% Triton X-100). Next, they were incubated for 1 h at RT in a humid chamber with primary antibodies against CENP-A (1:100; Abcam); ACA (1:20; MBL International Corp.); CENP-H (1:100; rabbit pAb; provided by K. Yoda); hRad21 (1:200; provided by F. Ishikawa, Kyoto University, Kyoto, Japan); hSgo1 (1:1,000); hMis12 (1:200); HP1-α, HP1-β, or HP1-γ (1:500; mAb 3584, 3448, or 3450; Millipore); p300 (1:500; mAb; Millipore); Vpr (1:400; rabbit pAb; TT144-1; Shimura et al., 1999); acetylated H3K9 (1:250; rabbit pAb; Cell Signaling Technology); and c-Myc (1:50; 9E10; Santa Cruz Biotechnology, Inc.). Primary antibodies were diluted in buffer A containing 10% goat serum. In the double staining of hRad21-myc and histone H2B-GFP, preparations were first stained for c-Myc for 30 min before anti-GFP antibody (1:50,000; MBL International Corp.) was applied for a further 30 min. After three washes in buffer A (once for 1 min and twice for 5 min), slides were next incubated with the secondary antibody Alexa Fluor 546–conjugated anti–mouse IgG (1:1,000; Invitrogen) or biotinylated anti–human IgG (1:500; Dako) and were then incubated for 30 min at RT in a humid chamber with streptavidin-FITC (1:500; Invitrogen), Alexa Fluor 546–conjugated anti–rabbit IgG (1:1,000; Invitrogen), Alexa Fluor 488–conjugated anti–rabbit IgG (1:400), or Alexa Fluor 488–conjugated anti–mouse IgG (1:400). The preparations were then washed three times (once for 1 min and twice for 5 min) and fixed in 4% PFA in buffer A for 15 min at RT. After being washed in PBS containing 1 mM PBS-EGTA, slides were stained with DAPI or Hoechst 33342 to visualize DNA. They were finally washed in PBS-EGTA for 5 min and mounted in antifade mounting medium (Kirkegaard and Perry Laboratories) before subsequent immunofluorescence microscopic analysis (see Immunofluorescence microscopy section).

Immunoprecipitation and HAT assay

To capture immunocomplexes, Dynabeads (Invitrogen) preincubated with either a mouse mAb against Vpr (8D1; Nakai-Murakami et al., 2007) or an anti-p300 pAb (N-15; Santa Cruz Biotechnology, Inc.), as well as mouse IgG (Sigma-Aldrich) or rabbit IgG (Sigma-Aldrich), were added to 1,000 µg cellular protein suspended in 250 µl lysis buffer. The resulting mixtures were incubated at 4°C overnight. The beads were then washed once with ice-cold buffer and boiled in sample buffer. The resulting immunocomplexes were analyzed using an anti-Vpr (8D1) mAb (1:1,000; Nakai-Murakami et al., 2007) or an anti-p300 pAb (1:100; N-15; input, 10% of the protein used in immunoprecipitation; Santa Cruz Biotechnology, Inc.). For HAT activity assays, Dynabeads coincubated with a mouse mAb against Flag (M2; Sigma-Aldrich) or a control mouse IgG were added to 1,000 µg cellular protein suspended in 250 µl lysis buffer, and the resulting mixtures were incubated at 4°C overnight. The beads were washed with ice-cold buffer and then with 1× HAT assay buffer (HAT assay kit; Millipore) according to the manufacturer's instructions. Next, a HAT assay cocktail containing 10 µg histone H3 (Millipore) and 100 µM acetyl-CoA (Sigma-Aldrich) was added to the beads, which were then incubated at 30°C in a shaking incubator for 30 min. Acetylation of histone H3 was assessed by Western blotting, performed using an antiacetylated histone H3 antibody (1:1,000; Cell Signaling Technology).

HAT activity

293T cells were transfected with Flag-EGFP, Flag-Vpr, or Flag-p300 (positive control). To capture immunocomplexes, Dynabeads conjugated with anti-Flag (M2) antibody (Sigma-Aldrich) or a control IgG (mouse mAb) were added, and the resulting mixtures were incubated at 4°C overnight. HAT activity was measured using a colorimetric assay (MBL International Corp.) according to the manufacturer's instructions. In brief, beads were washed with ice-cold TBS buffer. They were then mixed with a HAT substrate and incubated at 37°C in a shaking incubator for 3–6 h.

Statistical analysis

Statistical analyses were performed using a two-tailed unpaired *t* test. $P < 0.05$ was considered statistically significant.

Online supplemental material

Fig. S1 shows a PCS assay in two additional PBL donors, Vpr expression levels, and abnormal chromosome segregation in Vpr-expressing cells accompanying Videos 1–3. Fig. S2 shows the effects of Vpr expression on the interphase chromatin localization of hRad21 and HP1-α and an assessment of NIPBL in Vpr-induced PCS. Fig. S3 shows the specific down-regulation

of hSgo1, p300, and HP1-α/-γ protein expression by RNAi. Fig. S4 shows image analyses of chromatin-bound p300 and HP1-α in Vpr-expressing cells. Fig. S5 shows reduced dimethylation on histone H3 lysine 9 residue upon Vpr expression, the suppression of Vpr-associated HAT activity and localization of p300 in the presence of the HAT inhibitor, and the reduced frequency of PCS in cells expressing a Vpr protein carrying a mutated LR (p300 binding) domain. Videos 1–3 show mitosis in control (DOX^-; Video 1) and Vpr-expressing (DOX+; Videos 2 and 3) cells. Online supplemental material is available at http://www.jcb.org/cgi/content/full/jcb.201010118/DC1.

We thank Dr. F. Ishikawa for the hRad21 antibody, Drs. T. Hayakawa and T. Haraguchi for the HP1 antibodies, Dr. K. Kimura for the Smc1 and Smc3 antibodies, and Dr. Y. Watanabe for the hSgo1 antibody. We thank S. Fukushige and Y. Minemoto for technical support, A. Hori for statistical analyses, and Robert C. Miller and Saadi Khochbin for their help revising this manuscript.

This work was supported in part by Grants-in-Aid for Research on Advanced Medical Technology from the Ministry of Health, Labor, and Welfare, by the Japan Science and Technology Agency, and by funding from the Naito Foundation (to M. Shimura) and the Uehara Memorial Foundation (to Y. Toyoda).

Submitted: 25 October 2010
Accepted: 3 August 2011

References

Adams, R.R., M. Carmena, and W.C. Earnshaw. 2001. Chromosomal passengers and the (aurora) ABCs of mitosis. *Trends Cell Biol.* 11:49–54. doi:10.1016/S0962-8924(00)01880-8

Babu, J.R., K.B. Jeganathan, D.J. Baker, X. Wu, N. Kang-Decker, and J.M. van Deursen. 2003. Rae1 is an essential mitotic checkpoint regulator that cooperates with Bub3 to prevent chromosome missegregation. *J. Cell Biol.* 160:341–353. doi:10.1083/jcb.200211048

Boyes, J., P. Byfield, Y. Nakatani, and V. Ogryzko. 1998. Regulation of activity of the transcription factor GATA-1 by acetylation. *Nature*. 396:594–598. doi:10.1038/25166

Brady, T., L.M. Agosto, N. Malani, C.C. Berry, U. O'Doherty, and F. Bushman. 2009. HIV integration site distributions in resting and activated CD4+ T cells infected in culture. *AIDS*. 23:1461–1471. doi:10.1097/QAD.0b013e32832caf28

Caron, C., E. Col, and S. Khochbin. 2003. The viral control of cellular acetylation signaling. *Bioessays*. 25:58–65. doi:10.1002/bies.10202

Cereseto, A., L. Manganaro, M.I. Gutierrez, M. Terreni, A. Fittipaldi, M. Lusic, A. Marcello, and M. Giacca. 2005. Acetylation of HIV-1 integrase by p300 regulates viral integration. *EMBO J.* 24:3070–3081. doi:10.1038/sj.emboj.7600770

Chow, S.A., K.A. Vincent, V. Ellison, and P.O. Brown. 1992. Reversal of integration and DNA splicing mediated by integrase of human immunodeficiency virus. *Science*. 255:723–726. doi:10.1126/science.1738845

Cohen, E.A., E.F. Terwilliger, Y. Jalinoos, J. Proulx, J.G. Sodroski, and W.A. Haseltine. 1990. Identification of HIV-1 vpr product and function. *J. Acquir. Immune Defic. Syndr.* 3:11–18.

Connor, R.I., B.K. Chen, S. Choe, and N.R. Landau. 1995. Vpr is required for efficient replication of human immunodeficiency virus type-1 in mononuclear phagocytes. *Virology*. 206:935–944. doi:10.1006/viro.1995.1016

Corbeau, P., and J. Reynes. 2011. Immune reconstitution under antiretroviral therapy: the new challenge in HIV-1 infection. *Blood*. 117:5582–5590. doi:10.1182/blood-2010-12-322453

Debes, J.D., L.J. Schmidt, H. Huang, and D.J. Tindall. 2002. p300 mediates androgen-independent transactivation of the androgen receptor by interleukin 6. *Cancer Res.* 62:5632–5636.

Dorsett, D. 2007. Roles of the sister chromatid cohesion apparatus in gene expression, development, and human syndromes. *Chromosoma.* 116:1–13. doi:10.1007/s00412-006-0072-6

Felzien, L.K., C. Woffendin, M.O. Hottiger, R.A. Subbramanian, E.A. Cohen, and G.J. Nabel. 1998. HIV transcriptional activation by the accessory protein, VPR, is mediated by the p300 co-activator. *Proc. Natl. Acad. Sci. USA*. 95:5281–5286. doi:10.1073/pnas.95.9.5281

Fischle, W., B.S. Tseng, H.L. Dormann, B.M. Ueberheide, B.A. Garcia, J. Shabanowitz, D.F. Hunt, H. Funabiki, and C.D. Allis. 2005. Regulation of HP1-chromatin binding by histone H3 methylation and phosphorylation. *Nature*. 438:1116–1122. doi:10.1038/nature04219

Folks, T.M., J. Justement, A. Kinter, C.A. Dinarello, and A.S. Fauci. 1987. Cytokine-induced expression of HIV-1 in a chronically infected promonocyte cell line. *Science*. 238:800–802. doi:10.1126/science.3313729

Fouchier, R.A., B.E. Meyer, J.H. Simon, U. Fischer, and M.H. Malim. 1997. HIV-1 infection of non-dividing cells: evidence that the amino-terminal basic region of the viral matrix protein is important for Gag processing but not for post-entry nuclear import. *EMBO J.* 16:4531–4539. doi:10.1093/emboj/16.15.4531

Giménez-Abián, J.F., I. Sumara, T. Hirota, S. Hauf, D. Gerlich, C. de la Torre, J. Ellenberg, and J.M. Peters. 2004. Regulation of sister chromatid cohesion between chromosome arms. *Curr. Biol.* 14:1187–1193. doi:10.1016/j.cub.2004.06.052

Goshima, G., T. Kiyomitsu, K. Yoda, and M. Yanagida. 2003. Human centromere chromatin protein hMis12, essential for equal segregation, is independent of CENP-A loading pathway. *J. Cell Biol.* 160:25–39. doi:10.1083/jcb.200210005

Ha, G.H., H.S. Kim, C.G. Lee, H.Y. Park, E.J. Kim, H.J. Shin, J.C. Lee, K.W. Lee, and C.W. Lee. 2009. Mitotic catastrophe is the predominant response to histone acetyltransferase depletion. *Cell Death Differ.* 16:483–497. doi:10.1038/cdd.2008.182

Hayakawa, T., T. Haraguchi, H. Masumoto, and Y. Hiraoka. 2003. Cell cycle behavior of human HP1 subtypes: distinct molecular domains of HP1 are required for their centromeric localization during interphase and metaphase. *J. Cell Sci.* 116:3327–3338. doi:10.1242/jcs.00635

Hirano, T. 2005. SMC proteins and chromosome mechanics: from bacteria to humans. *Philos. Trans. R. Soc. Lond. B Biol. Sci.* 360:507–514. doi:10.1098/rstb.2004.1606

Hirota, T., J.J. Lipp, B.H. Toh, and J.M. Peters. 2005. Histone H3 serine 10 phosphorylation by Aurora B causes HP1 dissociation from heterochromatin. *Nature*. 438:1176–1180. doi:10.1038/nature04254

Hoque, M.T., and F. Ishikawa. 2002. Cohesin defects lead to premature sister chromatid separation, kinetochore dysfunction, and spindle-assembly checkpoint activation. *J. Biol. Chem.* 277:42306–42314. doi:10.1074/jbc.M206836200

Hoshino, S., B. Sun, M. Konishi, M. Shimura, T. Segawa, Y. Hagiwara, Y. Koyanagi, A. Iwamoto, J. Mimaya, H. Terunuma, et al. 2007. Vpr in plasma of HIV type 1-positive patients is correlated with the HIV type 1 RNA titers. *AIDS Res. Hum. Retroviruses*. 23:391–397. doi:10.1089/aid.2006.0124

Hottiger, M.O., and G.J. Nabel. 2000. Viral replication and the coactivators p300 and CBP. *Trends Microbiol.* 8:560–565. doi:10.1016/S0966-842X(00)01874-6

Inoue, A., J. Hyle, M.S. Lechner, and J.M. Lahti. 2008. Perturbation of HP1 localization and chromatin binding ability causes defects in sister-chromatid cohesion. *Mutat. Res.* 657:48–55.

Iwabu, Y., H. Fujita, M. Kinomoto, K. Kaneko, Y. Ishizaka, Y. Tanaka, T. Sata, and K. Tokunaga. 2009. HIV-1 accessory protein Vpu internalizes cell-surface BST-2/tetherin through transmembrane interactions leading to lysosomes. *J. Biol. Chem.* 284:35060–35072. doi:10.1074/jbc.M109.058305

Jenuwein, T., and C.D. Allis. 2001. Translating the histone code. *Science*. 293:1074–1080. doi:10.1126/science.1063127

Jeppesen, P., A. Mitchell, B. Turner, and P. Perry. 1992. Antibodies to defined histone epitopes reveal variations in chromatin conformation and underacetylation of centric heterochromatin in human metaphase chromosomes. *Chromosoma*. 101:322–332. doi:10.1007/BF00346011

Kajii, T., T. Ikeuchi, Z.Q. Yang, Y. Nakamura, Y. Tsuji, K. Yokomori, M. Kawamura, S. Fukuda, S. Horita, and A. Asamoto. 2001. Cancer-prone syndrome of mosaic variegated aneuploidy and total premature chromatid separation: report of five infants. *Am. J. Med. Genet.* 104:57–64. doi:10.1002/ajmg.1580

Kanda, T., K.F. Sullivan, and G.M. Wahl. 1998. Histone-GFP fusion protein enables sensitive analysis of chromosome dynamics in living mammalian cells. *Curr. Biol.* 8:377–385. doi:10.1016/S0960-9822(98)70156-3

Kaur, M., C. DeScipio, J. McCallum, D. Yaeger, M. Devoto, L.G. Jackson, N.B. Spinner, and I.D. Krantz. 2005. Precocious sister chromatid separation (PSCS) in Cornelia de Lange syndrome. *Am. J. Med. Genet. A.* 138:27–31.

Kawashima, S.A., T. Tsukahara, M. Langegger, S. Hauf, T.S. Kitajima, and Y. Watanabe. 2007. Shugoshin enables tension-generating attachment of kinetochores by loading Aurora to centromeres. *Genes Dev.* 21:420–435. doi:10.1101/gad.1497307

Kellum, R., and B.M. Alberts. 1995. Heterochromatin protein 1 is required for correct chromosome segregation in *Drosophila* embryos. *J. Cell Sci.* 108:1419–1431.

Kino, T., A. Gragerov, O. Slobodskaya, M. Tsopanomichalou, G.P. Chrousos, and G.N. Pavlakis. 2002. Human immunodeficiency virus type 1 (HIV-1) accessory protein Vpr induces transcription of the HIV-1 and glucocorticoid-responsive promoters by binding directly to p300/CBP coactivators. *J. Virol.* 76:9724–9734. doi:10.1128/JVI.76.19.9724-9734.2002

Kinomoto, M., T. Kanno, M. Shimura, Y. Ishizaka, A. Kojima, T. Kurata, T. Sata, and K. Tokunaga. 2007. All APOBEC3 family proteins differentially inhibit LINE-1 retrotransposition. *Nucleic Acids Res.* 35:2955–2964. doi:10.1093/nar/gkm181

Kitajima, T.S., T. Sakuno, K. Ishiguro, S. Iemura, T. Natsume, S.A. Kawashima, and Y. Watanabe. 2006. Shugoshin collaborates with protein phosphatase 2A to protect cohesin. *Nature*. 441:46–52. doi:10.1038/nature04663

Kiyomitsu, T., O. Iwasaki, C. Obuse, and M. Yanagida. 2010. Inner centromere formation requires hMis14, a trident kinetochore protein that specifically recruits HP1 to human chromosomes. *J. Cell Biol.* 188:791–807. doi:10.1083/jcb.200908096

Losada, A., M. Hirano, and T. Hirano. 2002. Cohesin release is required for sister chromatid resolution, but not for condensin-mediated compaction, at the onset of mitosis. *Genes Dev.* 16:3004–3016. doi:10.1101/gad.249202

Malim, M.H., and M. Emerman. 2008. HIV-1 accessory proteins—ensuring viral survival in a hostile environment. *Cell Host Microbe*. 3:388–398. doi:10.1016/j.chom.2008.04.008

Mantelingu, K., B.A. Reddy, V. Swaminathan, A.H. Kishore, N.B. Siddappa, G.V. Kumar, G. Nagashankar, N. Natesh, S. Roy, P.P. Sadhale, et al. 2007. Specific inhibition of p300-HAT alters global gene expression and represses HIV replication. *Chem. Biol.* 14:645–657. doi:10.1016/j.chembiol.2007.04.011

Marzio, G., M. Tyagi, M.I. Gutierrez, and M. Giacca. 1998. HIV-1 tat transactivator recruits p300 and CREB-binding protein histone acetyltransferases to the viral promoter. *Proc. Natl. Acad. Sci. USA*. 95:13519–13524. doi:10.1073/pnas.95.23.13519

Matalon, S., T.A. Rasmussen, and C.A. Dinarello. 2011. Histone deacetylase inhibitors for purging HIV-1 from the latent reservoir. *Mol. Med.* 17:466–472. doi:10.2119/molmed.2011.00076

Mateos-Langerak, J., M.C. Brink, M.S. Luijsterburg, I. van der Kraan, R. van Driel, and P.J. Verschure. 2007. Pericentromeric heterochromatin domains are maintained without accumulation of HP1. *Mol. Biol. Cell*. 18:1464–1471. doi:10.1091/mbc.E06-01-0025

McGuinness, B.E., T. Hirota, N.R. Kudo, J.M. Peters, and K. Nasmyth. 2005. Shugoshin prevents dissociation of cohesin from centromeres during mitosis in vertebrate cells. *PLoS Biol.* 3:e86. doi:10.1371/journal.pbio.0030086

Mermin, J., W. Were, J.P. Ekwaru, D. Moore, R. Downing, P. Behumbiize, J.R. Lule, A. Coutinho, J. Tappero, and R. Bunnell. 2008. Mortality in HIV-infected Ugandan adults receiving antiretroviral treatment and survival of their HIV-uninfected children: a prospective cohort study. *Lancet*. 371:752–759. doi:10.1016/S0140-6736(08)60345-1

Minc, E., Y. Allory, H.J. Worman, J.C. Courvalin, and B. Buendia. 1999. Localization and phosphorylation of HP1 proteins during the cell cycle in mammalian cells. *Chromosoma*. 108:220–234. doi:10.1007/s004120050372

Nakai-Murakami, C., M. Shimura, M. Kinomoto, Y. Takizawa, K. Tokunaga, T. Taguchi, S. Hoshino, K. Miyagawa, T. Sata, H. Kurumizaka, et al. 2007. HIV-1 Vpr induces ATM-dependent cellular signal with enhanced homologous recombination. *Oncogene*. 26:477–486. doi:10.1038/sj.onc.1209831

Nasmyth, K. 2002. Segregating sister genomes: the molecular biology of chromosome separation. *Science*. 297:559–565. doi:10.1126/science.1074757

Nonaka, N., T. Kitajima, S. Yokobayashi, G. Xiao, M. Yamamoto, S.I. Grewal, and Y. Watanabe. 2002. Recruitment of cohesin to heterochromatic regions by Swi6/HP1 in fission yeast. *Nat. Cell Biol.* 4:89–93. doi:10.1038/ncb739

Obuse, C., O. Iwasaki, T. Kiyomitsu, G. Goshima, Y. Toyoda, and M. Yanagida. 2004. A conserved Mis12 centromere complex is linked to heterochromatic HP1 and outer kinetochore protein Zwint-1. *Nat. Cell Biol.* 6:1135–1141. doi:10.1038/ncb1187

Pidoux, A.L., and R.C. Allshire. 2004. Kinetochore and heterochromatin domains of the fission yeast centromere. *Chromosome Res.* 12:521–534. doi:10.1023/B:CHRO.0000036586.81775.8b

Pouwels, J., A.M. Kukkonen, W. Lan, J.R. Daum, G.J. Gorbsky, T. Stukenberg, and M.J. Kallio. 2007. Shugoshin 1 plays a central role in kinetochore assembly and is required for kinetochore targeting of Plk1. *Cell Cycle*. 6:1579–1585. doi:10.4161/cc.6.13.4442

Remboutsika, E., Y. Lutz, A. Gansmuller, J.L. Vonesch, R. Losson, and P. Chambon. 1999. The putative nuclear receptor mediator TIF1alpha is tightly associated with euchromatin. *J. Cell Sci.* 112:1671–1683.

Serrano, A., M. Rodríguez-Corsino, and A. Losada. 2009. Heterochromatin protein 1 (HP1) proteins do not drive pericentromeric cohesin enrichment in human cells. *PLoS ONE*. 4:e5118. doi:10.1371/journal.pone.0005118

Shimura, M., Y. Tanaka, S. Nakamura, Y. Minemoto, K. Yamashita, K. Hatake, F. Takaku, and Y. Ishizaka. 1999. Micronuclei formation and aneuploidy induced by Vpr, an accessory gene of human immunodeficiency virus type 1. *FASEB J.* 13:621–637.

Shimura, M., K. Tokunaga, M. Konishi, Y. Sato, C. Kobayashi, T. Sata, and Y. Ishizaka. 2005. Premature sister chromatid separation in HIV-1-infected peripheral blood lymphocytes. *AIDS*. 19:1434–1438. doi:10.1097/01.aids.0000180788.92627.e7

Sotillo, R., E. Hernando, E. Díaz-Rodríguez, J. Teruya-Feldstein, C. Cordón-Cardo, S.W. Lowe, and R. Benezra. 2007. Mad2 overexpression promotes aneuploidy and tumorigenesis in mice. *Cancer Cell*. 11:9–23. doi:10.1016/j.ccr.2006.10.019

Sumara, I., E. Vorlaufer, P.T. Stukenberg, O. Kelm, N. Redemann, E.A. Nigg, and J.M. Peters. 2002. The dissociation of cohesin from chromosomes in prophase is regulated by Polo-like kinase. *Mol. Cell*. 9:515–525. doi:10.1016/S1097-2765(02)00473-2

Thompson, P.W., S.V. Davies, and J.A. Whittaker. 1993. C-anaphase in a case of acute nonlymphocytic leukemia. *Cancer Genet. Cytogenet.* 71:148–150. doi:10.1016/0165-4608(93)90021-D

Todorov, I.T., A. Attaran, and S.E. Kearsey. 1995. BM28, a human member of the MCM2-3-5 family, is displaced from chromatin during DNA replication. *J. Cell Biol.* 129:1433–1445. doi:10.1083/jcb.129.6.1433

Toyoda, Y., and M. Yanagida. 2006. Coordinated requirements of human topo II and cohesin for metaphase centromere alignment under Mad2-dependent spindle checkpoint surveillance. *Mol. Biol. Cell*. 17:2287–2302. doi:10.1091/mbc.E05-11-1089

Vagnarelli, P.B., and W.C. Earnshaw. 2001. INCENP loss from an inactive centromere correlates with the loss of sister chromatid cohesion. *Chromosoma*. 110:393–401. doi:10.1007/s004120100163

Vega, H., Q. Waisfisz, M. Gordillo, N. Sakai, I. Yanagihara, M. Yamada, D. van Gosliga, H. Kayserili, C. Xu, K. Ozono, et al. 2005. Roberts syndrome is caused by mutations in *ESCO2*, a human homolog of yeast *ECO1* that is essential for the establishment of sister chromatid cohesion. *Nat. Genet.* 37:468–470. doi:10.1038/ng1548

Waizenegger, I.C., S. Hauf, A. Meinke, and J.M. Peters. 2000. Two distinct pathways remove mammalian cohesin from chromosome arms in prophase and from centromeres in anaphase. *Cell*. 103:399–410. doi:10.1016/S0092-8674(00)00132-X

Williams, S.A., L.F. Chen, H. Kwon, C.M. Ruiz-Jarabo, E. Verdin, and W.C. Greene. 2006. NF-kappaB p50 promotes HIV latency through HDAC recruitment and repression of transcriptional initiation. *EMBO J.* 25:139–149. doi:10.1038/sj.emboj.7600900

Yamagishi, Y., T. Sakuno, M. Shimura, and Y. Watanabe. 2008. Heterochromatin links to centromeric protection by recruiting shugoshin. *Nature*. 455:251–255. doi:10.1038/nature07217

Yanagida, M. 2005. Basic mechanism of eukaryotic chromosome segregation. *Philos. Trans. R. Soc. Lond. B Biol. Sci.* 360:609–621. doi:10.1098/rstb.2004.1615

Zhang, N., G. Ge, R. Meyer, S. Sethi, D. Basu, S. Pradhan, Y.J. Zhao, X.N. Li, W.W. Cai, A.K. El-Naggar, et al. 2008. Overexpression of Separase induces aneuploidy and mammary tumorigenesis. *Proc. Natl. Acad. Sci. USA*. 105:13033–13038. doi:10.1073/pnas.0801610105

Zhu, D., M.S. Ma, R.Z. Zhao, and M.Y. Li. 1995. Centromere spreading and centromeric aberrations in ovarian tumors. *Cancer Genet. Cytogenet.* 80:63–65. doi:10.1016/0165-4608(94)00128-X